Available online at www.sciencedirect.com

ScienceDirect

Nuclear Physics B 935 (2018) 17–39

NUCLEAR PHYSICS B

www.elsevier.com/locate/nuclphysb

Anatomy of $B_s \to VV$ decays and effects of next-to-leading order contributions in the perturbative QCD factorization approach

Da-Cheng Yan [a], Xin Liu [b], Zhen-Jun Xiao [a,c,*]

[a] *Department of Physics and Institute of Theoretical Physics, Nanjing Normal University, Nanjing, Jiangsu 210023, China*

[b] *School of Physics and Electronic Engineering, Jiangsu Normal University, Xuzhou 221116, China*

[c] *Jiangsu Key Laboratory for Numerical Simulation of Large Scale Complex Systems, Nanjing Normal University, Nanjing, Jiangsu 210023, China*

Received 5 July 2018; accepted 4 August 2018
Available online 13 August 2018
Editor: Hong-Jian He

Abstract

By employing the perturbative QCD (PQCD) factorization approach, we calculated the branching ratios, CP-violating asymmetries, the longitudinal and transverse polarization fractions and other physical observables of the thirteen charmless hadronic $\bar{B}_s^0 \to VV$ decays with the inclusion of all currently known next-to-leading order (NLO) contributions. We focused on the examination of the effects of all those currently known NLO contributions and found that: (a) for the measured decays $\bar{B}_s^0 \to \phi\phi, K^{*0}\phi, \bar{K}^{*0}K^{*0}$ and $\rho^0\phi$, the NLO contributions can provide $\sim 20\%$ to $\sim 40\%$ enhancements to the leading order (LO) PQCD predictions of their CP-averaged branching ratios, and consequently the agreement between the PQCD predictions and the measured values are improved effectively after the inclusion of the NLO contributions; (b) for the measured decays, the NLO corrections to the LO PQCD predictions for $(f_L, f_\perp)$ and $(\phi_\parallel, \phi_\perp)$ are generally small in size, but the weak penguin annihilation contributions play an important role in understanding the data about their decay rates, f_L and $f_\perp$; (c) the NLO PQCD predictions for above mentioned physical observables do agree with the measured ones and the theoretical predictions from the QCDF, SCET and FAT approaches; (d) for other considered $B_s^0 \to VV$ decays, the NLO PQCD predictions for their decay rates and other physical observables are also basically consistent with the theoretical

* Corresponding author.
E-mail addresses: 1019453259@qq.com (D.-C. Yan), liuxin@jsnu.edu.cn (X. Liu), xiaozhenjun@njnu.edu.cn (Z.-J. Xiao).

https://doi.org/10.1016/j.nuclphysb.2018.08.002

predictions from other popular approaches, future precision measurements could help us to test or examine these predictions.

1. Introduction

During the past three decades, the two-body charmless hadronic $B_s \to VV$ decays, with V being the light vector mesons ρ, K^*, ϕ and ω, have been studied by many authors based on rather different factorization approaches [1–11]. Several such decay modes, such as $B_s^0 \to \phi\phi$ decay, have been observed by CDF and LHCb experiments [12–21]. When compared with the similar $B_s \to PP$, PV (here $P = \pi$, K, η, and η') decays, $B_s \to VV$ are indeed much more complicated due to the fact that more helicity amplitudes should be taken into account. The $B_s \to VV$ decays can offer, consequently, rich opportunities for us to test the Stand Model (SM) and to search for the exotic new physics beyond the SM.

Experimentally, a large transverse polarization fraction of $B \to \phi K^*$ was firstly observed in 2003 by BABAR and Belle Collaborations [22]. The new world averages of f_L as given by HFAG-2016 [21] for $B \to (\phi, \rho, \omega)$ decays, for example, are the following:

$$f_L(B^+ \to VK^{*+}) = \begin{cases} 0.50 \pm 0.05\,, & \text{for } V = \phi, \\ 0.78 \pm 0.12\,, & \text{for } V = \rho^0, \\ 0.41 \pm 0.19\,, & \text{for } V = \omega, \end{cases} \tag{1}$$

$$f_L(B^0 \to VK^{*0}) = \begin{cases} 0.497 \pm 0.017\,, & \text{for } V = \phi, \\ 0.40 \pm 0.14\,, & \text{for } V = \rho^0, \\ 0.70 \pm 0.13\,, & \text{for } V = \omega. \end{cases} \tag{2}$$

These measured values were in strong confliction with the general expectation $f_L \approx 1$ in the naive factorization ansatz [23], which is the so-called "polarization puzzle" [24–27]. The similar deviations also be observed later for $B^+ \to \phi(K_1, K_2^*)$ and ωK_2^* decays [21,28].

For the charmless $B_s^0 \to VV$ decays studied in this paper, the similar puzzles have also been observed by CDF and LHCb Collaboration for $\bar{B}_s^0 \to \phi\phi$, $K^*\phi$ and $K^{*0}\bar{K}^{*0}$ decay modes [12–17]. The new world averages of f_L and $f_\perp$ as given by HFAG-2016 [21] for these three decay modes are the following:

$$\bar{B}_s^0 \to \phi\phi: \qquad f_L = 0.361 \pm 0.022, \quad f_\perp = 0.306 \pm 0.023, \tag{3}$$

$$\bar{B}_s^0 \to K^*\phi: \qquad f_L = 0.51 \pm 0.17, \quad f_\perp = 0.28 \pm 0.12, \tag{4}$$

$$\bar{B}_s^0 \to K^{*0}\overline{K}^{*0}: \qquad f_L = 0.201 \pm 0.070, \quad f_\perp = 0.38 \pm 0.11. \tag{5}$$

More measurements are expected in the near future.

Theoretically, a number of strategies were proposed to resolve the above mentioned "polarization puzzle" within and/or beyond the SM. For example, the weak penguin annihilation contributions in QCD factorization (QCDF) approach was proposed by Kagan [29], the final state interactions were considered in Refs. [24,30,31], the form-factor tuning in the perturbative QCD (PQCD) approach was suggested by Li [26], and even the exotic new physics effects have been studied by authors in Refs. [32,33]. Obviously, it is hard to get a good answer to this seemingly long-standing puzzle at present. However, according to the statement in Ref. [27], the

complicated QCD dynamics involved in such $B/B_s \to VV$ decays should be fully explored before resorting to the possible new physics beyond the SM. Therefore, the QCDF approach [1–5,34], the soft-collinear effective theory (SCET) [10,11] and the PQCD approach [7–9,35–37], have been adopted to investigate these kinds of decays systematically.

The two-body charmless hadronic decays $B_s \to VV$ have been systematically studied in the PQCD approach at leading order (LO) in 2007 [8]. Recently, the authors of Ref. [9] made improved estimations for the $B_{(s)} \to VV$ modes by keeping the terms with the higher power of the ratios $r_{2,3} = m_{V_{2,3}}/m_{B_{(s)}}$ in the PQCD approach, with $m_{B_{(s)}}$ and $m_{V_{2,3}}$ being the masses of the initial and final states. However, there still existed some issues to be clarified, e.g. the measured large decay rates for $B_s \to \phi K^*$ and $\bar{K}^{*0}K^{*0}$ decays, the latest measurement of a smaller f_L for $B_s \to \bar{K}^{*0}K^{*0}$ decay, etc.

Therefore, we would like to revisit those two-body charmless $B_s \to VV$ decays by taking into account all currently known next-to-leading order (NLO) contributions in the PQCD factorization approach. We will focus on the effects of the NLO contributions arising from various possible sources, such as the QCD vertex corrections (VC), the quark loops (QL), and the chromomagnetic penguins [38,39] in the SM. As can be seen from Refs. [38–42], the NLO contributions do play an important role in understanding the known anomalies of B physics such as the amazingly large $B \to K\eta'$ decay rates [41,42], the longitudinal-polarization dominated $B^0 \to \rho^0\rho^0$ [38] and the evidently nonzero $\Delta A_{K\pi}$, i.e., the famous "$K\pi$-puzzle" [39,40], and so forth. Very recently, we extend these calculations to the cases such as $B_s^0 \to (K\pi, KK)$ decays [43], $B_s^0 \to (\pi\eta^{(\prime)}, \eta^{(\prime)}\eta^{(\prime)})$ decays [44] and $B_s^0 \to PV$ decays [45]. We found that the currently known NLO contributions can interfere with the LO part constructively or destructively for those considered B_s meson decay modes. Consequently, the agreement between the PQCD predictions and the experimental measurements of the CP-averaged branching ratios, the polarization fractions and CP-violating asymmetries was indeed improved effectively due to the inclusion of the NLO contributions.

This paper is organized as follows. In Sec. 2, we shall present various decay amplitudes for the considered decay modes in the PQCD approach at the LO and NLO level. We show the PQCD predictions and several phenomenological analyses for the branching ratios, CP-violating asymmetries and polarization observables of thirteen $B_s \to VV$ decays in Sec 3. A short summary is given in Sec. 4.

2. Decay amplitudes at LO and NLO level

We treat the B_s meson as a heavy-light system and consider it at rest for simplicity. By employing the light-cone coordinates, we define the B_s meson with momentum P_1, the emitted meson M_2 with the momentum P_2 along the direction of $n = (1, 0, \mathbf{0}_{\rm T})$, and the recoiled meson M_3 with the momentum P_3 in the direction of $v = (0, 1, \mathbf{0}_{\rm T})$ (here, n and v are the light-like dimensionless vectors), respectively, as the following,

$$P_1 = \frac{m_{B_s}}{\sqrt{2}}(1, 1, \mathbf{0}_{\rm T}), \quad P_2 = \frac{M_{B_s}}{\sqrt{2}}(1 - r_3^2, r_2^2, \mathbf{0}_{\rm T}), \quad P_3 = \frac{M_{B_s}}{\sqrt{2}}(r_3^2, 1 - r_2^2, \mathbf{0}_{\rm T}). \tag{6}$$

The polarization vectors of the final states can then be parametrized as:

$$\epsilon_2^L = \frac{1}{\sqrt{2}r_2}(1 - r_3^2, -r_2^2, \mathbf{0}_{\rm T}), \qquad \epsilon_3^L = \frac{1}{\sqrt{2}r_3}(-r_3^2, 1 - r_2^2, \mathbf{0}_{\rm T}),$$
$$\epsilon_2^T = (0, 0, \mathbf{1}_{\rm T}), \qquad \epsilon_3^T = (0, 0, \mathbf{1}_{\rm T}), \tag{7}$$

with $\epsilon^{L(T)}$ being the longitudinal (transverse) polarization vector.

The momenta k_i $(i = 1, 2, 3)$ carried by the light anti-quark in the initial B_s and final $V_{2,3}$ mesons are chosen as follows:

$$k_1 = (x_1, 0, \mathbf{k}_{1\mathrm{T}}), \quad k_2 = (x_2(1 - r_3^2), x_2 r_2^2, \mathbf{k}_{2\mathrm{T}}), \quad k_3 = (x_3 r_3^2, x_3(1 - r_2^2), \mathbf{k}_{3\mathrm{T}}). \tag{8}$$

The integration over $k_{1,2}^-$ and k_3^+ will lead conceptually to the decay amplitudes in the PQCD approach,

$$\mathcal{A}(B_s^0 \to V_2 V_3) \sim \int dx_1 dx_2 dx_3 b_1 db_1 b_2 db_2 b_3 db_3 \times \mathrm{Tr}\Big[C(t)\Phi_{B_s}(x_1, b_1)\Phi_{V_2}(x_2, b_2)\Phi_{V_3}(x_3, b_3) H(x_i, b_i, t) S_t(x_i)\, e^{-S(t)}\Big], \tag{9}$$

in which, b is the conjugate space coordinate of transverse momentum k_{T}, $C(t)$ stands for the Wilson coefficients evaluated at the scale t, and Φ denotes the hadron wave functions, which are nonperturbative but universal inputs, of the initial and final states. The kernel $H(x_i, b_i, t)$ describes the hard dynamics associated with the effective "six-quark interaction" exchanged by a hard gluon. The Sudakov factors $e^{-S(t)}$ and $S_t(x_i)$ together suppress the soft dynamics in the endpoint region effectively [46].

2.1. Wave functions and decay amplitudes

Without the endpoint singularities in the evaluations, the hadron wave functions are the only input in the PQCD approach. These nonperturbative quantities are process independent and could be obtained with the techniques of QCD sum rule and/or Lattice QCD, or be fitted to the measurements with good precision.

For B_s meson, its wave function could be adopted with the Lorentz structure [8,9]

$$\Phi_{B_s} = \frac{1}{\sqrt{6}}(\not{P}_{B_s} + m_{B_s})\gamma_5 \phi_{B_s}(\mathbf{k}), \tag{10}$$

in which the distribution amplitude ϕ_{B_s} is modeled as

$$\phi_{B_s}(x, b) = N_{B_s} x^2(1 - x)^2 \exp\left[-\frac{m_{B_s}^2\, x^2}{2\omega_{B_s}^2} - \frac{1}{2}(\omega_{B_s} b)^2\right], \tag{11}$$

with ω_{B_s} being the shape parameter. We take $\omega_{B_s} = 0.50 \pm 0.05$ GeV for the B_s meson based on the studies of lattice QCD and light-cone sum rule [47–49]. The normalization factor N_{B_s} will be determined through the normalization condition: $\int \phi_{B_s}(x, b = 0)dx = f_{B_s}/(2\sqrt{6})$ with the decay constant $f_{B_s} = 0.23$ GeV.

For the vector meson, the longitudinally and transversely polarized wave functions up to twist-3 are given by [49,50]

$$\begin{aligned}
\Phi_V^L &= \frac{1}{\sqrt{6}}\left[m_V \not{\epsilon}_L \phi_V(x) + \not{\epsilon}_L \not{P} \phi_V^t(x) + m_V \phi_V^s(x)\right] \\
\Phi_V^\perp &= \frac{1}{\sqrt{6}}\left[m_V \not{\epsilon}_T \phi_V^v(x) + \not{\epsilon}_T \not{P} \phi_V^T(x) + m_V i\epsilon_{\mu\nu\rho\sigma}\gamma_5\gamma^\mu \epsilon_T^\nu n^\rho v^\sigma \phi_V^a(x)\right],
\end{aligned} \tag{12}$$

where P and m_V are the momentum and the mass of the light vector mesons, and $\epsilon_{L(T)}$ is the corresponding longitudinal (transverse) polarization vector [37]. Here $\epsilon_{\mu\nu\rho\sigma}$ is Levi-Civita tensor with the convention $\epsilon^{0123} = 1$.

The twist-2 distribution amplitudes $\phi_V(x)$ and $\phi_V^T(x)$ can be written in the following form [49,50]

$$\phi_V(x) = \frac{3f_V}{\sqrt{6}} x(1-x)\left[1 + a_{1V}^{\parallel} C_1^{3/2}(t) + a_{2V}^{\parallel} C_2^{3/2}(t)\right], \tag{13}$$

$$\phi_V^T(x) = \frac{3f_V^T}{\sqrt{6}} x(1-x)\left[1 + a_{1V}^{\perp} C_1^{3/2}(t) + a_{2V}^{\perp} C_2^{3/2}(t)\right], \tag{14}$$

where $t = 2x-1$, $f_V^{(T)}$ is the decay constants of the vector meson with longitudinal (transverse) polarization. The Gegenbauer moments here are the same as those in Refs. [49–51]:

$$\begin{aligned}
&a_{1\rho}^{\parallel(\perp)} = a_{1\omega}^{\parallel(\perp)} = a_{1\phi}^{\parallel(\perp)} = 0,\ \ a_{1K^*}^{\parallel(\perp)} = 0.03 \pm 0.02\,(0.04 \pm 0.03)\,,\\
&a_{2\rho}^{\parallel(\perp)} = a_{2\omega}^{\parallel(\perp)} = 0.15 \pm 0.07\,(0.14 \pm 0.06)\ a_{2\phi}^{\parallel(\perp)} = 0\,(0.20 \pm 0.07)\,,\\
&a_{2K^*}^{\parallel(\perp)} = 0.11 \pm 0.09\,(0.10 \pm 0.08)\,.
\end{aligned} \tag{15}$$

For the twist-3 distribution amplitudes, for simplicity, we adopt the asymptotic forms [8,9]

$$\begin{aligned}
&\phi_V^t(x) = \frac{3f_V^T}{2\sqrt{6}} t^2,\ \ \phi_V^s(x) = \frac{3f_V^T}{2\sqrt{6}}(-t),\\
&\phi_V^v(x) = \frac{3f_V}{8\sqrt{6}}(1+t^2),\ \ \phi_V^a(x) = \frac{3f_V}{4\sqrt{6}}(-t).
\end{aligned} \tag{16}$$

The above choices of vector-meson distribution amplitudes can essentially explain the polarization fractions of the measured $B \to K^*\phi$, $B \to K^*\rho$ and $B \to \rho\rho$ decays [26,27,35], together with the right branching ratios.

2.2. Example of the LO decay amplitudes

In the SM, for the considered $\bar{B}_s^0 \to VV$ decays induced by the $b \to q$ transition with $q = (d, s)$, the weak effective Hamiltonian H_{eff} can be written as [52],

$$H_{eff} = \frac{G_F}{\sqrt{2}}\left\{ V_{ub}V_{uq}^*\left[C_1(\mu)O_1^u(\mu) + C_2(\mu)O_2^u(\mu)\right] - V_{tb}V_{tq}^*\left[\sum_{i=3}^{10} C_i(\mu)O_i(\mu)\right]\right\} + \text{h.c.} \tag{17}$$

where the Fermi constant $G_F = 1.16639 \times 10^{-5}$ GeV^{-2}, and V_{ij} is the Cabbibo–Kobayashi–Maskawa (CKM) matrix element, $C_i(\mu)$ are the Wilson coefficients and $O_i(\mu)$ are the local four-quark operators. For convenience, the combinations a_i of the Wilson coefficients are defined as usual [8,9]:

$$\begin{aligned}
&a_1 = C_2 + C_1/3, \quad a_2 = C_1 + C_2/3,\\
&a_i = C_i + C_{i\pm1}/3,\ (i = 3-10)\,,
\end{aligned} \tag{18}$$

where the upper (lower) sign applies, when i is odd (even).

At leading order, as illustrated in Fig. 1, there are eight types of Feynman diagrams contributing to the $\bar{B}_s^0 \to VV$ decays, which can be classified into three types: the factorizable emission diagrams (Fig. 1(a) and 1(b)); the nonfactorizable emission diagrams (Fig. 1(c) and 1(d)); and

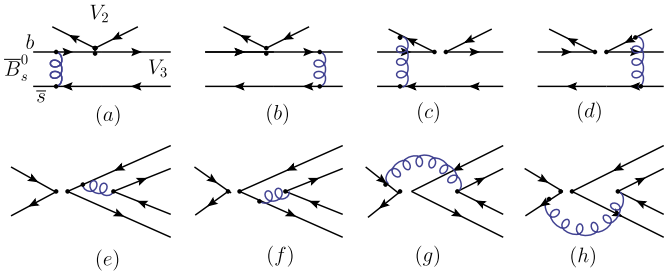

Fig. 1. Typical Feynman diagrams of $\bar{B}_s^0 \to VV$ decays at leading order.

the annihilation diagrams (Fig. 1(e)–1(h)). As mentioned in the Introduction, the considered thirteen $\bar{B}_s^0 \to VV$ modes have been studied at LO in the PQCD approach [8,9]. The factorization formulas of decay amplitudes with various topologies have been presented explicitly in Ref. [8]. Therefore, after the confirmation by our independent recalculations, we shall not collect those analytic expressions here for simplicity. In this work, we aim to examine the effects of all currently known NLO contributions to the considered $\bar{B}_s^0 \to VV$ decay modes in the PQCD approach to see whether one can improve the consistency between the theory and the experiment in the SM or not, which would be helpful for us to judge the necessity of the exotic new physics beyond the SM.

For $\bar{B}_s^0 \to VV$ decays, both of the longitudinal and transverse polarizations will contribute. Then, the decay amplitudes can be decomposed into three parts [9]:

$$\mathcal{A}(\epsilon_2, \epsilon_3) = i\mathcal{A}^L + i(\epsilon_2^T \cdot \epsilon_3^T)\mathcal{A}^N + (\epsilon_{\mu\nu\alpha\beta} n^\mu v^\nu \epsilon_2^{T\alpha} \epsilon_3^{T\beta})\mathcal{A}^T, \tag{19}$$

where $\mathcal{A}^L, \mathcal{A}^N$ and $\mathcal{A}^T$ correspond to the longitudinally, normally and transversely polarized amplitudes, respectively, whose detailed expressions can be inferred from Refs. [8,9].

2.3. NLO contributions

In the framework of the PQCD approach, many two-body charmless $B/B_s \to PP, PV$ decays have been investigated by including currently known NLO contributions, for example, in Refs. [39–45,53,54]. Of course, some NLO contributions are still not known at present, as discussed in Ref. [41]. The currently known NLO corrections to the LO PQCD predictions of $B_s \to VV$ decays are the following:

(a) The NLO Wilson coefficients $C_i(m_W)$ (NLO-WC), the renormalization group running matrix $U(m_1, m_2, \alpha)$ at NLO level and the strong coupling constant $\alpha_s(\mu)$ at two-loop level as presented in Ref. [52];
(b) The NLO contributions from the vertex corrections (VC) [38,39] as illustrated in Figs. 2(a)–2(d);
(c) The NLO contributions from the quark-loops (QL) [38,39] as shown in Figs. 2(e)–2(f);
(d) The NLO contributions from the chromo-magnetic penguin (MP) operator O_{8g} [38,39,55] as illustrated in Figs. 2(g)–2(h).

In this paper, we adopt directly the formulas for all currently known NLO contributions from Refs. [38–44,55] without further discussions about the details. Moreover, some essential com-

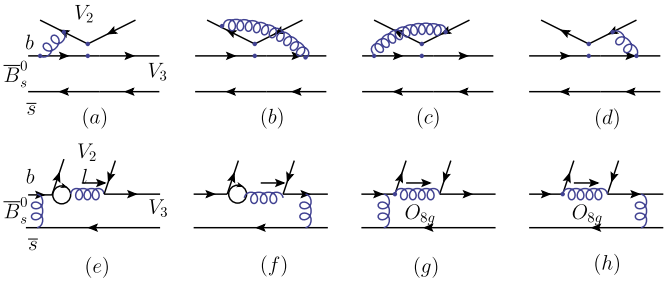

Fig. 2. Feynman diagrams for NLO contributions: the vertex corrections (a–d); the quark-loop contributions (e–f) and the chromomagnetic penguin contributions (g–h).

ments should be given for those still unknown NLO corrections to the nonfactorizable emission amplitudes and the annihilation amplitudes as follows:

(a) For the nonfactorizable emission diagrams as shown in Fig. 1, since the hard gluons are emitted from the upper quark line of Fig. 1(c) and the upper anti-quark line of Fig. 1(d) respectively, the contribution from these two figures will be strongly canceled each other, the remaining contribution is therefore becoming rather small in magnitude. In NLO level, another suppression factor $\alpha_s(t)$ will appear, the resultant NLO contribution from the hard-spectators should become much smaller than the dominant contribution from the "tree" emission diagrams (Fig. 1(a) and 1(b)).
(b) For the annihilation diagrams as shown in Fig. 1(e)–1(h), the corresponding NLO contributions are in fact doubly suppressed by the factors $1/m_{B_s}$ and $\alpha_s(t)$, and consequently must become much smaller than those dominant LO contribution from Fig. 1(a) and 1(b).

Therefore, it is reasonable for us to expect that those still unknown NLO contributions in the PQCD approach are in fact the higher order corrections to the already small LO pieces, and should be much smaller than the dominant contribution for the considered decays, say less than 5% of the dominant ones.

According to Refs. [38,39], the vertex corrections can be absorbed into the redefinition of the Wilson coefficients $a_i(\mu)$ by adding a vertex-function $V_i(M)$ to them.

$$\begin{aligned} a_{1,2}(\mu) &\to a_{1,2}(\mu) + \frac{\alpha_s(\mu)}{9\pi}\, C_{1,2}(\mu)\, V_{1,2}(M)\,, \\ a_i(\mu) &\to a_i(\mu) + \frac{\alpha_s(\mu)}{9\pi}\, C_{i+1}(\mu)\, V_i(M), \qquad \text{for } i = 3,5,7,9, \\ a_j(\mu) &\to a_j(\mu) + \frac{\alpha_s(\mu)}{9\pi}\, C_{j-1}(\mu)\, V_j(M), \qquad \text{for } j = 4,6,8,10, \end{aligned} \tag{20}$$

where M denotes the vector meson emitted from the weak vertex (i.e. the M_2 in Fig. 2(a)–2(d)). The expressions of the vertex-functions $V_i(M)$ with both longitudinal and transverse components can be found easily in Refs. [56,57].

The NLO "Quark-Loop" and "Magnetic-Penguin" contributions are in fact a kind of penguin corrections with insertion of the four-quark operators and the chromo-magnetic operator O_{8g}, respectively, as shown in Figs. 2(e,f) and 2(g,h). For the $b \to s$ transition, for example, the corresponding effective Hamiltonian H_{eff}^{ql} and H_{eff}^{mp} can be written in the following form:

$$H_{eff}^{(ql)} = -\sum_{q=u,c,t}\sum_{q'}\frac{G_F}{\sqrt{2}}V_{qb}^*V_{qs}\frac{\alpha_s(\mu)}{2\pi}C^q(\mu,l^2)\left[\bar{b}\gamma_\rho\,(1-\gamma_5)\,T^a s\right]\left(\bar{q}'\gamma^\rho T^a q'\right), \tag{21}$$

$$H_{eff}^{mp} = -\frac{G_F}{\sqrt{2}}\frac{g_s}{8\pi^2}m_b\,V_{tb}^*V_{ts}\,C_{8g}^{eff}\,\bar{s}_i\,\sigma^{\mu\nu}\,(1+\gamma_5)\,T_{ij}^a\,G_{\mu\nu}^a\,b_j, \tag{22}$$

where l^2 is the invariant mass of the gluon which attaches the quark loops in Figs. 2(e,f), and the functions $C^q(\mu,l^2)$ can be inferred from Refs. [38–42]. The C_{8g}^{eff} in Eq. (22) is an effective Wilson coefficient with the definition of $C_{8g}^{eff} = C_{8g} + C_5$ [52].

With explicit evaluations, we find the following three points:

(1) For the pure annihilation decays of $B_s^0 \to \rho\rho$, $\rho\omega$ and $\omega\omega$, they do not receive the NLO contributions from the vertex corrections, the quark-loop and the magnetic-penguin diagrams. The NLO correction to these decay modes comes only from the NLO-WCs and the strong coupling constant $\alpha_s(\mu)$ at the two-loop level.

(2) For the $B_s^0 \to \rho^0\phi$ and $\omega\phi$ channels with only $B_s \to \phi$ transition and no annihilation diagrams, the "quark-loop" and "magnetic-penguin" diagrams cannot contribute to these two decay modes. The related NLO contributions are mainly induced by the vertex corrections to the emitted ρ or ω mesons.

(3) For the remaining seven decay modes, besides the LO decay amplitudes, all of the currently known NLO contributions should be taken into account as follows:

$$\begin{aligned}
&\mathcal{A}^{(u),i}_{\rho^0K^{*0}} \to \mathcal{A}^{(u),i}_{\rho^0K^{*0}} + \mathcal{M}^{(u,c),i}_{\rho^0K^{*0}}\,,\\
&\mathcal{A}^{(t),i}_{\rho^0K^{*0}} \to \mathcal{A}^{(t),i}_{\rho^0K^{*0}} - \mathcal{M}^{(t),i}_{\rho^0K^{*0}} - \mathcal{M}^{(g),i}_{\rho^0K^{*0}}\,,\\
&\mathcal{A}^{(u),i}_{\rho^-K^{*+}} \to \mathcal{A}^{(u),i}_{\rho^-K^{*+}} + \mathcal{M}^{(u,c),i}_{\rho^-K^{*+}}\,,\\
&\mathcal{A}^{(t),i}_{\rho^-K^{*+}} \to \mathcal{A}^{(t),i}_{\rho^-K^{*+}} - \mathcal{M}^{(t),i}_{\rho^-K^{*+}} - \mathcal{M}^{(g),i}_{\rho^-K^{*+}}\,,\\
&\mathcal{A}^{(u),i}_{\omega K^{*0}} \to \mathcal{A}^{(u),i}_{\omega K^{*0}} + \mathcal{M}^{(u,c),i}_{\omega K^{*0}}\,,\\
&\mathcal{A}^{(t),i}_{\omega K^{*0}} \to \mathcal{A}^{(t),i}_{\omega K^{*0}} - \mathcal{M}^{(t),i}_{\omega K^{*0}} - \mathcal{M}^{(g),i}_{\omega K^{*0}}\,,\\
&\mathcal{A}^{(u),i}_{\phi K^{*0}} \to \mathcal{A}^{(u),i}_{\phi K^{*0}} + \mathcal{M}^{(u,c),i}_{\phi K^{*0}}\,,\\
&\mathcal{A}^{(t),i}_{\phi K^{*0}} \to \mathcal{A}^{(t),i}_{\phi K^{*0}} - \mathcal{M}^{(t),i}_{\phi K^{*0}} - \mathcal{M}^{(g),i}_{\phi K^{*0}}\,,\\
&\mathcal{A}^{(u),i}_{K^{*-}K^{*+}} \to \mathcal{A}^{(u),i}_{K^{*-}K^{*+}} + \mathcal{M}^{(u,c),i}_{K^{*-}K^{*+}}\,,\\
&\mathcal{A}^{(t),i}_{K^{*-}K^{*+}} \to \mathcal{A}^{(t),i}_{K^{*-}K^{*+}} - \mathcal{M}^{(t),i}_{K^{*-}K^{*+}} - \mathcal{M}^{(g),i}_{K^{*-}K^{*+}}\,,\\
&\mathcal{A}^{(u),i}_{K^{*0}\bar{K}^{*0}} \to \mathcal{A}^{(u),i}_{K^{*0}\bar{K}^{*0}} + \mathcal{M}^{(u,c),i}_{K^{*0}\bar{K}^{*0}}\,,\\
&\mathcal{A}^{(t),i}_{K^{*0}\bar{K}^{*0}} \to \mathcal{A}^{(t),i}_{K^{*0}\bar{K}^{*0}} - \mathcal{M}^{(t),i}_{K^{*0}\bar{K}^{*0}} - \mathcal{M}^{(g),i}_{K^{*0}\bar{K}^{*0}}\,,\\
&\mathcal{A}^{(u),i}_{\phi\phi} \to \mathcal{A}^{(u),i}_{\phi\phi} + \mathcal{M}^{(u,c),i}_{\phi\phi}\,,\\
&\mathcal{A}^{(t),i}_{\phi\phi} \to \mathcal{A}^{(t),i}_{\phi\phi} - \mathcal{M}^{(t),i}_{\phi\phi} - \mathcal{M}^{(g),i}_{\phi\phi}\,,
\end{aligned} \tag{23}$$

where $i = L, N, T$ and the terms $\mathcal{A}^{(u,t),i}_{V_2V_3}$ stand for the LO amplitudes, while $\mathcal{M}^{(u,c,t),i}_{V_2V_3}$ and $\mathcal{M}^{(g),i}_{V_2V_3}$ are the NLO ones, which describe the NLO contributions arising from the up-loop, charm-loop, QCD-penguin-loop, and magnetic-penguin diagrams, respectively.

Now, we can calculate the decay amplitudes $\mathcal{M}^{(ql),i}_{V_2V_3}$ and $\mathcal{M}^{(mp),i}_{V_2V_3}$ in the PQCD approach. As mentioned in Eq. (19), for $B_s \to VV$ decays, there are three individual polarization amplitudes $\mathcal{M}^{L,N,T}_{V_2V_3}$. For the longitudinal components, the NLO decay amplitudes $\mathcal{M}^{(ql),L}_{V_2V_3}$ and $\mathcal{M}^{(mp),L}_{V_2V_3}$ can be written as:

$$\begin{aligned}
\mathcal{M}^{(ql),L}_{V_2V_3} = -8m^4_{B_s}\frac{C_F^2}{\sqrt{6}}\int_0^1 dx_1dx_2dx_3\int_0^\infty b_1db_1b_3db_3\,\phi_{B_s}(x_1,b_1)\Big\{&[(1+x_3)\phi_2(x_2)\phi_3(x_3)\\
&-2r_2\phi_2^s(x_2)\phi_3(x_3)+r_3(1-2x_3)\phi_2(x_2)(\phi_3^s(x_3)+\phi_3^t(x_3))\\
&-2r_2r_3\phi_2^s(x_2)((2+x_3)\phi_3^s(x_3)-x_3\phi_3^t(x_3))]\\
&\cdot\alpha_s^2(t_a)\cdot h_e(x_1,x_3,b_1,b_3)\cdot\exp[-S_{ab}(t_a)]\;C^{(q)}(t_a,l^2)\\
&+[2r_3\phi_2(x_2)\phi_3^s(x_3)-4r_2r_3\phi_2^s(x_2)]\phi_3^s(x_3)\cdot\alpha_s^2(t_b)\cdot h_e(x_3,x_1,b_3,b_1)\\
&\cdot\exp[-S_{ab}(t_b)]\,C^{(q)}(t_b,l'^2)\Big\},
\end{aligned}\tag{24}$$

$$\begin{aligned}
\mathcal{M}^{(mp),L}_{V_2V_3} = 8m^6_{B_s}\frac{C_F^2}{\sqrt{6}}\int_0^1 dx_1dx_2dx_3\int_0^\infty b_1db_1b_2db_2b_3db_3\,\phi_{B_s}(x_1,b_1)\\
\times\Big\{\Big[(-1+x_3)\big[2\phi_3(x_3)-r_3(x_3-1)\phi_3^t(x_3)+r_3(x_3+3)\phi_3^s(x_3)\big]\phi_2(x_2)\\
+\;r_2x_2(3\phi_2^s(x_2)-\phi_2^t(x_2))\big[(1+x_3)\phi_3(x_3)-r_3(2x_3-1)(\phi_3^s(x_3)+\phi_3^t(x_3))\big]\\
+\;r_2r_3(x_3-1)(3\phi_2^s(x_2)+\phi_2^t(x_2))(\phi_3^t(x_3)-\phi_3^s(x_3))\Big]\\
\cdot\alpha_s^2(t_a)h_g(x_i,b_i)\cdot\exp[-S_{cd}(t_a)]\,C_{8g}^{eff}(t_a)\\
-\big[4r_3\phi_2(x_2)-2r_2r_3x_2(3\phi_2^s(x_2)-\phi_2^t(x_2))\big]\phi_3^s(x_3)\\
\cdot\alpha_s^2(t_b)\cdot h_g'(x_i,b_i)\cdot\exp[-S_{cd}(t_b)]\cdot C_{8g}^{eff}(t_b)\Big\},
\end{aligned}\tag{25}$$

with $C_F = 4/3$.

The transverse components $\mathcal{M}^{(ql),N,T}_{V_2V_3}$ and $\mathcal{M}^{(mp),N,T}_{V_2V_3}$ of the corresponding decay amplitudes can be written in the form of

$$\begin{aligned}
\mathcal{M}^{(ql),N}_{V_2V_3} = -8m^4_{B_s}r_2\frac{C_F^2}{\sqrt{6}}\int_0^1 dx_1dx_2dx_3\int_0^\infty b_1db_1b_3db_3\,\phi_{B_s}(x_1,b_1)\\
\times\Big\{\Big[\phi_3^T(x_3)(\phi_2^a(x_2)+\phi_2^v(x_2))+r_3(x_3+2)(\phi_2^a(x_2)\phi_3^a(x_3)+\phi_2^v(x_2)\phi_3^v(x_3))\\
-\;r_3x_3(\phi_2^a(x_2)\phi_3^v(x_3)+\phi_2^v(x_2)\phi_3^a(x_3))\Big]\\
\cdot\alpha_s^2(t_a)\cdot h_e(x_1,x_3,b_1,b_3)\cdot\exp[-S_{ab}(t_a)]\;C^{(q)}(t_a,l^2)\\
+\big[r_2r_3(\phi_2^a(x_2)\phi_3^a(x_3)+\phi_2^a(x_2)\phi_3^v(x_3)+\phi_2^v(x_2)\phi_3^a(x_3)\\
+\;\phi_2^v(x_2)\phi_3^v(x_3))\big]\phi_3^s(x_3)\\
\cdot\alpha_s^2(t_b)\cdot h_e(x_3,x_1,b_3,b_1)\cdot\exp[-S_{ab}(t_b)]\,C^{(q)}(t_b,l'^2)\Big\},
\end{aligned}\tag{26}$$

$$\mathcal{M}^{(ql),T}_{V_2V_3} = -8m_{B_s}^4 r_2 \frac{C_F^2}{\sqrt{6}} \int_0^1 dx_1 dx_2 dx_3 \int_0^\infty b_1 db_1 b_3 db_3\, \phi_{B_s}(x_1, b_1)$$
$$\times \Big\{ \Big[\phi_3^T(x_3)(\phi_2^a(x_2) + \phi_2^v(x_2)) + r_3(x_3+2)(\phi_2^a(x_2)\phi_3^v(x_3) + \phi_2^v(x_2)\phi_3^a(x_3))$$
$$- r_3 x_3 (\phi_2^a(x_2)\phi_3^a(x_3) + \phi_2^v(x_2)\phi_3^v(x_3)) \Big]$$
$$\cdot \alpha_s^2(t_a) \cdot h_e(x_1, x_3, b_1, b_3) \cdot \exp\left[-S_{ab}(t_a)\right]\, C^{(q)}(t_a, l^2)$$
$$+ \Big[r_2 r_3 (\phi_2^a(x_2)\phi_3^a(x_3) + \phi_2^a(x_2)\phi_3^v(x_3) + \phi_2^v(x_2)\phi_3^a(x_3)$$
$$+ \phi_2^v(x_2)\phi_3^v(x_3)) \Big] \phi_3^s(x_3)$$
$$\cdot \alpha_s^2(t_b) \cdot h_e(x_3, x_1, b_3, b_1) \cdot \exp[-S_{ab}(t_b)]\, C^{(q)}(t_b, l'^2) \Big\}, \tag{27}$$

$$\mathcal{M}^{(mp),N}_{V_2V_3} = 8m_{B_s}^6 \frac{C_F^2}{\sqrt{6}} \int_0^1 dx_1 dx_2 dx_3 \int_0^\infty b_1 db_1 b_2 db_2 b_3 db_3\, \phi_{B_s}(x_1, b_1)$$
$$\times \Big\{ \Big[-r_3(x_3^2 - 1)\phi_2^T(x_2)(\phi_3^a(x_3) - \phi_3^v(x_3))$$
$$- r_2 x_2 (1 + x_3)\phi_3^T(x_3)(\phi_2^a(x_2) - \phi_2^v(x_2))$$
$$+ r_2 r_3 (2x_2 x_3 - x_2 + x_3 - 1)(\phi_2^a(x_2)\phi_3^a(x_3) + \phi_2^v(x_2)\phi_3^v(x_3))$$
$$+ r_2 r_3 (2x_2 x_3 - x_2 - x_3 - 1)(\phi_2^a(x_2)\phi_3^v(x_3) + \phi_2^v(x_2)\phi_3^a(x_3)) \Big]$$
$$\cdot \alpha_s^2(t_a) h_g(x_i, b_i) \cdot \exp[-S_{cd}(t_a)]\, C_{8g}^{eff}(t_a)$$
$$- \Big[r_2 r_3 x_2 (\phi_2^a(x_2) + \phi_2^v(x_2))(\phi_3^a(x_3) + \phi_3^v(x_3)) \Big]$$
$$\cdot \alpha_s^2(t_b) \cdot h'_g(x_i, b_i) \cdot \exp[-S_{cd}(t_b)] \cdot C_{8g}^{eff}(t_b) \Big\}, \tag{28}$$

$$\mathcal{M}^{(mp),T}_{V_2V_3} = 8m_{B_s}^6 \frac{C_F^2}{\sqrt{6}} \int_0^1 dx_1 dx_2 dx_3 \int_0^\infty b_1 db_1 b_2 db_2 b_3 db_3\, \phi_{B_s}(x_1, b_1)$$
$$\times \Big\{ \Big[-r_3(x_3^2 - 1)\phi_2^T(x_2)(\phi_3^a(x_3) - \phi_3^v(x_3))$$
$$- r_2 x_2 (1 + x_3)\phi_3^T(x_3) \left(\phi_2^a(x_2) - \phi_2^v(x_2)\right)$$
$$+ r_2 r_3 (2x_2 x_3 - x_2 + x_3 - 1) \left(\phi_2^a(x_2)\phi_3^v(x_3) + \phi_2^v(x_2)\phi_3^a(x_3)\right)$$
$$+ r_2 r_3 (2x_2 x_3 - x_2 - x_3 - 1) \left(\phi_2^a(x_2)\phi_3^a(x_3) + \phi_2^v(x_2)\phi_3^v(x_3)\right) \Big]$$
$$\cdot \alpha_s^2(t_a) h_g(x_i, b_i) \cdot \exp[-S_{cd}(t_a)]\, C_{8g}^{eff}(t_a)$$
$$- \Big[r_2 r_3 x_2 (\phi_2^a(x_2) + \phi_2^v(x_2)) \left(\phi_3^a(x_3) + \phi_3^v(x_3)\right) \Big]$$
$$\cdot \alpha_s^2(t_b) \cdot h'_g(x_i, b_i) \cdot \exp[-S_{cd}(t_b)] \cdot C_{8g}^{eff}(t_b) \Big\}. \tag{29}$$

In the above equations, the explicit expressions for the hard functions (h_e, h_g, h'_g), the functions $C^{(q)}(t_a, l^2)$ and $C^{(q)}(t_b, l'^2)$, the Sudakov factors $S_{ab}(t)$ and $S_{cd}(t)$, the hard scales $t_{a,b}$ and the effective Wilson coefficients $C_{8g}^{eff}(t)$, can be found easily, for example, in Refs. [38–44].

3. Numerical results

In the numerical calculations, the following input parameters will be used implicitly. The masses, decay constants and QCD scales are in units of GeV [9,20]

$$\begin{aligned}
&\Lambda_{\overline{\rm MS}}^{(f=5)} = 0.225, \quad f_{B_s} = 0.23, \quad f_\rho = 0.216, \quad f_\rho^T = 0.165,\\
&f_\omega = 0.187, \quad f_\omega^T = 0.151,\\
&M_{B_s} = 5.37, \quad f_\phi = 0.215, \quad f_\phi^T = 0.186, \quad f_{K^*} = 0.220,\\
&f_{K^*}^T = 0.185, \quad m_{K^*} = 0.892,\\
&m_\phi = 1.02, \quad m_\rho = 0.77, \quad m_\omega = 0.78, \quad \tau_{B_s^0} = 1.497\ \text{ps},\\
&m_b = 4.8, \quad M_W = 80.42.
\end{aligned} \tag{30}$$

For the CKM matrix elements, we adopt the Wolfenstein parametrization up to $\mathcal{O}(\lambda^5)$ with the updated parameters as [20]

$$\begin{aligned}
&\lambda = 0.22537 \pm 0.00061, \quad A = 0.814^{+0.023}_{-0.024}, \quad \bar\rho = 0.117 \pm 0.021,\\
&\bar\eta = 0.353 \pm 0.013.
\end{aligned} \tag{31}$$

The total decay amplitude for $\bar B_s^0 \to VV$ decays can be expressed as

$$|\,\mathcal{M}(\bar B_s^0 \to f)\,|^2 = |\,\mathcal{A}_0\,|^2 + |\,\mathcal{A}_\parallel\,|^2 + |\,\mathcal{A}_\perp\,|^2 \tag{32}$$

where $\mathcal{A}_0, \mathcal{A}_\parallel, \mathcal{A}_\perp$ denote the longitudinal, parallel, and perpendicular polarization amplitude in the transversity basis, respectively, which are defined as follows [9]:

$$A_0 = \mathcal{A}_L, \quad A_\parallel = \sqrt{2}\mathcal{A}^N, \quad A_\perp = \sqrt{2}\mathcal{A}^T. \tag{33}$$

Therefore, the CP-averaged branching ratio can be written as

$$BR = \frac{|\mathbf{P}|}{16\pi M_B^2}\tau_{B_s}\left[|\,\mathcal{M}(\bar B_s^0 \to f)\,|^2 + |\,\mathcal{M}(B_s^0 \to \bar f)\,|^2\right], \tag{34}$$

where $\mathbf{P}$ is the 3-momentum of either of the two vector mesons in the final state and τ_{B_s} is the lifetime of the B_s meson.

The definitions of the polarization fractions $f_{L,\parallel,\perp}$ and the relative phases $\phi_{\parallel,\perp}$ are given as

$$f_{L,\parallel,\perp} = \frac{|\,A_{L,\parallel,\perp}\,|^2}{|\,A_0\,|^2 + |\,A_\parallel\,|^2 + |\,A_\perp\,|^2}, \qquad \phi_{\parallel,\perp} = \text{Arg}(A_{\parallel,\perp}/A_0). \tag{35}$$

Combined with the CP-conjugated decay, the direct CP asymmetry can be defined as

$$\begin{aligned}
A_{CP}^{\rm dir} &= \frac{BR(\bar B_s^0 \to f) - BR(B_s^0 \to \bar f)}{BR(\bar B_s^0 \to f) + BR(B_s^0 \to \bar f)}\\
&= \frac{|\,\mathcal{M}(\bar B_s^0 \to f)\,|^2 - |\,\mathcal{M}(B_s^0 \to \bar f)\,|^2}{|\,\mathcal{M}(\bar B_s^0 \to f)\,|^2 + |\,\mathcal{M}(B_s^0 \to \bar f)\,|^2}.
\end{aligned} \tag{36}$$

Besides, we also evaluate the following observables:

$$\begin{aligned}
&A_{CP}^0 = \frac{f_L - \bar f_L}{f_L + \bar f_L}, \quad A_{CP}^\perp = \frac{f_\perp - \bar f_\perp}{f_\perp + \bar f_\perp},\\
&\Delta\phi_\parallel = \frac{\phi_\parallel - \bar\phi_\parallel}{2}, \quad \Delta\phi_\perp = \frac{\phi_\perp - \bar\phi_\perp}{2}.
\end{aligned} \tag{37}$$

Table 1
The predicted branching ratios (in units of 10^{-6}) of the $\bar{B}_s^0 \to \phi\phi$, $K^{*0}\phi$, and $\bar{K}^{*0}K^{*0}$ decays in the PQCD approach at LO and NLO level. As a comparison, the numerical results from the previous PQCD, QCDF, SCET, and FAT approaches are also quoted.

Modes	LO	NLOWC	+VC	+QL	+MP	NLO
$\bar{B}_s^0 \to \phi\phi$	16.4	19.8	17.6	21.2	15.2	$18.8^{+4.9}_{-3.8}$
$\bar{B}_s^0 \to K^{*0}\phi$	0.38	0.46	0.42	0.60	0.34	$0.42^{+0.13}_{-0.10}$
$\bar{B}_s^0 \to \bar{K}^{*0}K^{*0}$	5.0	6.61	7.16	8.68	4.70	$6.68^{+2.9}_{-2.2}$
Modes	PQCD [9]	QCDF [3]	QCDF [2]	SCET [10]	FAT [58]	Data [14,16,18]
$\bar{B}_s^0 \to \phi\phi$	$16.7^{+4.9}_{-3.8}$	$16.7^{+11.9}_{-9.1}$	$21.8^{+30.4}_{-17.1}$	19.0 ± 6.5	26.4 ± 7.6	18.4 ± 1.9
$\bar{B}_s^0 \to K^{*0}\phi$	$0.39^{+0.20}_{-0.17}$	$0.37^{+0.25}_{-0.21}$	$0.4^{+0.51}_{-0.31}$	0.56 ± 0.19	0.7 ± 0.18	1.13 ± 0.30
$\bar{B}_s^0 \to \bar{K}^{*0}K^{*0}$	$5.4^{+3.0}_{-2.4}$	6.6 ± 2.2	$9.1^{+11.3}_{-6.8}$	8.6 ± 3.1	14.9 ± 3.6	10.8 ± 2.84

Table 2
Same as Table 1 but for the longitudinal f_L (the first entry) and perpendicular $f_\perp$ (the second entry) polarization fractions (%).

Modes	LO	NLOWC	+VC	+QL	+MP	NLO
$\bar{B}_s^0 \to \phi\phi$	31.2	37.3	27.0	50.4	23.9	$31.6^{+6.7}_{-5.3}$
	33.2	30.1	37.9	23.8	36.6	$35.5^{+2.8}_{-4.2}$
$\bar{B}_s^0 \to K^{*0}\phi$	46.2	53.2	46.8	62.8	37.6	$47.1^{+8.2}_{-7.4}$
	26.7	23.1	28.6	18.4	30.8	$28.3^{+3.4}_{-2.8}$
$\bar{B}_s^0 \to \bar{K}^{*0}K^{*0}$	35.7	45.4	49.0	57.5	25.2	$43.4^{+12.7}_{-12.9}$
	28.2	25.4	22.8	19.7	35.3	$23.5^{+5.8}_{-5.9}$
Modes	PQCD [9]	QCDF [3]	QCDF [2]	SCET [10]	FAT [58]	Data [12–14,18]
$\bar{B}_s^0 \to \phi\phi$	$34.7^{+8.9}_{-7.1}$	$36.2^{+23.2}_{-18.4}$	43^{+1}_{-34}	51 ± 16.4	39.7 ± 16.0	34.8 ± 4.6
	$31.6^{+3.5}_{-4.4}$	–	–	22.2 ± 9.9	31.2 ± 8.9	36.5 ± 5.2
$\bar{B}_s^0 \to K^{*0}\phi$	$50.0^{+8.1}_{-7.2}$	$43^{+21.1}_{-18.1}$	40^{+67}_{-35}	54.6 ± 16.0	38.9 ± 14.7	51 ± 16.5
	$24.2^{+3.6}_{-3.9}$	–	–	20.5 ± 9.1	31.4 ± 8.1	28 ± 11.2
$\bar{B}_s^0 \to \bar{K}^{*0}K^{*0}$	$38.3^{+12.1}_{-10.5}$	$56^{+22.4}_{-26.1}$	63^{+42}_{-29}	44.9 ± 18.3	34.3 ± 12.6	20.1 ± 6.9
	$30.0^{+5.3}_{-6.1}$	–	–	24.9 ± 11.1	33.2 ± 6.9	38 ± 11.4

In Tables 1–10, we present our numerical results for the branching ratios, the direct CP asymmetries, and the polarization observables of the thirteen $\bar{B}_s^0 \to VV$ decays. Besides, the dominant contributions to these decays are also listed in the tables through the symbols "T" (the color-allowed tree contributions), "C" (the color-suppressed tree contributions), "P" (penguin contributions), and "A" (the annihilation contributions). The label "LO" denote the PQCD predictions at the leading order only. The label "NLOWC" means the LO results with the NLO Wilson coefficients, and "+VC", "+QL", "+MP", and "NLO" mean the inclusions of the vertex corrections, the quark loops, the magnetic penguin, and all the above NLO corrections, respec-

Table 3
The PQCD predictions for the branching ratios, f_L (%) and $f_\perp$ (%) for the relevant decays. The data are taken from Refs. [12–14,16,18]. The meaning of the labels are described in the text.

Mode	Br (10^{-6})			f_L (%)			$f_\perp$ (%)		
	NLO	No Ann	Data	NLO	No Ann	Data	NLO	No Ann	Data
$\bar{B}_s^0 \to \phi\phi$	$18.8^{+4.9}_{-3.8}$	$7.6^{+4.9}_{-3.8}$	18.4 ± 1.9	$31.6^{+6.7}_{-5.3}$	$78.2^{+3.8}_{-3.1}$	34.8 ± 4.6	$35.5^{+2.8}_{-4.2}$	$12.7^{+2.6}_{-3.0}$	36.5 ± 5.2
$\bar{B}_s^0 \to K^{*0}\phi$	$0.42^{+0.13}_{-0.10}$	$0.15^{+0.05}_{-0.03}$	1.13 ± 0.30	$47.1^{+8.2}_{-7.4}$	$80.8^{+5.3}_{-5.1}$	51 ± 16.5	$28.3^{+3.4}_{-2.8}$	$11.6^{+3.1}_{-3.6}$	28 ± 11.2
$\bar{B}_s^0 \to \bar{K}^{*0}K^{*0}$	$6.68^{+2.9}_{-2.2}$	$4.86^{+1.5}_{-1.2}$	10.8 ± 2.84	$46.4^{+12.7}_{-12.9}$	$89.6^{+3.2}_{-2.7}$	20.1 ± 6.9	$23.5^{+5.8}_{-5.9}$	$3.6^{+1.5}_{-1.3}$	38 ± 11.4

Table 4
The PQCD predictions for the relative phase $\phi_\parallel$ (the first row) and $\phi_\perp$ (the second row) of the three measured $\bar{B}_s^0 \to \phi\phi, K^{*0}\phi, \bar{K}^{*0}K^{*0}$ decays. For comparison, we also cite the theoretical predictions in the previous PQCD [9], SCET [10] and FAT [58] approaches. The experimental data are taken from the Refs. [15,18].

Mode	LO	NLO	PQCD [9]	SCET [10]	FAT [58]	Data
$\bar{B}_s^0 \to \phi\phi$	2.07	$1.65^{+0.20}_{-0.13}$	2.01 ± 0.23	2.41 ± 0.62	2.53 ± 0.28	2.54 ± 0.11
	2.10	$1.69^{+0.22}_{-0.12}$	$2.00^{+0.24}_{-0.21}$	2.54 ± 0.62	2.56 ± 0.27	2.67 ± 0.23
$\bar{B}_s^0 \to K^{*0}\phi$	1.98	$1.62^{+0.22}_{-0.18}$	$1.95^{+0.21}_{-0.22}$	2.37 ± 0.59	2.52 ± 0.27	1.75 ± 0.58
	1.98	$1.65^{+0.17}_{-0.14}$	$1.95^{+0.21}_{-0.22}$	2.50 ± 0.59	2.55 ± 0.27	
$\bar{B}_s^0 \to \bar{K}^{*0}K^{*0}$	2.12	$1.84^{+0.25}_{-0.20}$	$2.12^{+0.21}_{-0.25}$	2.47 ± 0.67	2.10 ± 0.23	
	2.15	$1.89^{+0.22}_{-0.21}$	$2.15^{+0.22}_{-0.23}$	2.60 ± 0.67	2.10 ± 0.23	

Table 5
The PQCD predictions for the direct CP asymmetries $\mathcal{A}_{CP}^{\rm dir}$ (%) of $\bar{B}_s^0 \to \phi\phi, K^{*0}\phi, \bar{K}^{*0}K^{*0}$ decays.

Mode	Class	LO	NLO	$\rm PQCD_{LO}$ [9]	QCDF [3]	SCET [10]	FAT [58]
$\bar{B}_s^0 \to \phi\phi$	P	0	0.7 ± 0.2	0	$0.2^{+0.6}_{-0.3}$	-0.39 ± 0.44	0.83 ± 0.28
$\bar{B}_s^0 \to K^{*0}\phi$	P	0	$-15.9^{+2.7}_{-2.0}$	0	-9^{+5}_{-6}	6.6 ± 7.6	-17.3 ± 5.6
$\bar{B}_s^0 \to \bar{K}^{*0}K^{*0}$	P	0	0.7 ± 0.2	0	$0.4^{+0.1}_{-0.6}$	-0.56 ± 0.61	0.78 ± 0.19

tively. In Table 3, we also test the effects of the contributions from the annihilation diagrams, and the label "No Ann" means the full NLO contributions except for the annihilation contributions. For comparison, the experimental measurements [12–18] and the numerical results arising from the former PQCD [9], QCDF [2,3], SCET [10] and Factorization-Assisted Topological-Amplitude Approach (FAT) [58] are also presented in these tables. The theoretical errors mainly come from the uncertainties of various input parameters, in particular, the dominant ones from the shape parameter $\omega_{B_s} = 0.50 \pm 0.05$, $f_{B_s} = 0.23 \pm 0.02$ GeV and the Gegenbauer moments in the distribution amplitudes of light vector mesons. The total errors of the NLO PQCD predictions are given in the Tables by adding the individual uncertainties in quadrature.

Among the thirteen $B_s^0 \to VV$ decays considered in this work, only three of them, namely, $\bar{B}_s^0 \to \phi\phi$, $\bar{B}_s^0 \to K^{*0}\phi$ and $\bar{B}_s^0 \to \bar{K}^{*0}K^{*0}$, have been well measured by experiments up to now. The measured values of the branching ratios, $(f_L, f_\perp)$ and $(\phi_\parallel, \phi_\perp)$, can be found easily in

Table 6
The PQCD predictions for CP-averaged branching ratios (in units of 10^{-6}) of the ten $\bar{B}_s^0 \to VV$ decays.

Mode	Class	LO	NLO	PQCD [9]	QCDF [3]	SCET [10]	FAT [58]
$\bar{B}_s^0 \to K^{*+}\rho^-$	T	23.2	$20.6^{+9.2}_{-6.9}$	$24.0^{+11.1}_{-9.4}$	$21.6^{+1.8}_{-3.5}$	28.1 ± 4.2	38.6 ± 8.27
$\bar{B}_s^0 \to K^{*0}\rho^0$	C	0.38	$0.69^{+0.21}_{-0.16}$	$0.40^{+0.24}_{-0.17}$	$1.3^{+3.2}_{-0.7}$	1.04 ± 0.3	1.18 ± 0.46
$\bar{B}_s^0 \to K^{*0}\omega$	C	0.33	$0.66^{+0.20}_{-0.18}$	$0.35^{+0.19}_{-0.20}$	$1.1^{+2.4}_{-0.6}$	0.41 ± 0.14	0.97 ± 0.38
$\bar{B}_s^0 \to K^{*+}K^{*-}$	P	5.02	$6.50^{+2.8}_{-2.1}$	$5.4^{+3.3}_{-2.5}$	$7.6^{+2.5}_{-2.7}$	11.0 ± 3.3	15.9 ± 3.5
$\bar{B}_s^0 \to \omega\phi$	P	0.19	$0.22^{+0.15}_{-0.10}$	$0.17^{+0.21}_{-0.08}$	$0.18^{+0.13}_{-0.06}$	0.04 ± 0.01	3.69 ± 1.45
$\bar{B}_s^0 \to \rho^0\phi$	P	0.21	$0.25^{+0.18}_{-0.11}$	$0.23^{+0.15}_{-0.06}$	$0.18^{+0.8}_{-0.13}$	0.36 ± 0.05	0.07 ± 0.03
$\bar{B}_s^0 \to \omega\rho^0$	A	0.009	0.007	0.009	0.004	–	0.08 ± 0.05
$\bar{B}_s^0 \to \rho^+\rho^-$	A	1.65	$1.70^{+0.6}_{-0.5}$	$1.5^{+0.7}_{-0.6}$	$0.68^{+0.7}_{-0.5}$	–	0.10 ± 0.06
$\bar{B}_s^0 \to \rho^0\rho^0$	A	0.82	$0.90^{+0.6}_{-0.5}$	$0.74^{+0.7}_{-0.6}$	$0.34^{+0.4}_{-0.3}$	–	0.05 ± 0.03
$\bar{B}_s^0 \to \omega\omega$	A	0.45	$0.50^{+0.18}_{-0.16}$	$0.40^{+0.21}_{-0.23}$	$0.19^{+0.21}_{-0.15}$	–	0.03 ± 0.02

Table 7
The PQCD predictions for the longitudinal polarization fractions f_L (%) of the remaining ten $\bar{B}_s^0 \to VV$ decays.

Mode	Class	LO	NLO	PQCD [9]	QCDF [3]	SCET [10]	FAT [58]
$\bar{B}_s^0 \to K^{*+}\rho^-$	T	93.4	$94.1^{+1.0}_{-1.0}$	$95^{+1.4}_{-1.4}$	$92^{+1.4}_{-3.6}$	99.1 ± 0.3	94.4 ± 1.2
$\bar{B}_s^0 \to K^{*0}\rho^0$	C	50.1	$83.4^{+4.8}_{-4.8}$	$57^{+8.1}_{-15.7}$	$90^{+5.0}_{-24.0}$	87 ± 5	79.8 ± 8.0
$\bar{B}_s^0 \to K^{*0}\omega$	C	51.7	$82.7^{+5.4}_{-5.3}$	$50^{+13.1}_{-17.0}$	$90^{+4.2}_{-23.2}$	64 ± 15	77.9 ± 9.2
$\bar{B}_s^0 \to K^{*+}K^{*-}$	P	40.2	$48.1^{+9.7}_{-8.9}$	$42^{+14.2}_{-11.2}$	$52^{+20.2}_{-21.6}$	55 ± 14	30.9 ± 10.4
$\bar{B}_s^0 \to \omega\phi$	P	65.7	$55.2^{+6.6}_{-4.7}$	$69^{+11.2}_{-12.6}$	$95^{+1.0}_{-42.1}$	100	–
$\bar{B}_s^0 \to \rho^0\phi$	P	84.5	$90.2^{+1.2}_{-1.5}$	$86^{+1.4}_{-1.4}$	$88^{+2.2}_{-18.0}$	100	–
$\bar{B}_s^0 \to \rho^+\rho^-$	A	~ 100	~ 100	~ 100	~ 100	–	–
$\bar{B}_s^0 \to \rho^0\rho^0$	A	~ 100	~ 100	~ 100	~ 100	–	–
$\bar{B}_s^0 \to \omega\omega$	A	~ 100	~ 100	~ 100	~ 100	–	–
$\bar{B}_s^0 \to \omega\rho^0$	A	~ 100	~ 100	~ 100	~ 100	–	–

Table 1–4. For $\bar{B}_s^0 \to \rho^0\phi$ decay, however, only its branching ratio has been reported by LHCb Collaboration very recently [17]:

$$Br(\bar{B}_s^0 \to \rho^0\phi) = (0.27 \pm 0.08) \times 10^{-6}, \tag{38}$$

and other physical parameters are still unknown at present. On the basis of the data and the theoretical predictions in different approaches/methods, some remarks are in order:

(1) Generally speaking, the $\bar{B}_s^0 \to \phi\phi$ and $\bar{B}_s^0 \to \bar{K}^{*0}K^{*0}$, and the $\bar{B}_s^0 \to K^{*0}\phi$ decays are governed by the QCD penguin contributions through the $b \to s$ and $b \to d$ transition, respectively. Then the former two CKM-favored modes have larger decay rates than the latter CKM-suppressed one due to $|V_{ts}/V_{td}|^2 \sim 21$, which can be easily seen from the Table 1. The evident deviations between the branching ratios of the two $\Delta S = 1$ channels, i.e., $B_s^0 \to \phi\phi$

Table 8
The PQCD predictions for the direct CP asymmetries $\mathcal{A}_{CP}^{\rm dir}$ (%) of the all thirteen $\bar{B}_s^0 \to VV$ decays.

Mode	Class	LO	NLO	$\rm PQCD_{LO}$ [9]	QCDF [3]	SCET [10]	FAT [58]
$\bar{B}_s^0 \to K^{*+}\rho^-$	T	-8.5	$-13.7^{+3.3}_{-2.8}$	$-9.1^{+1.7}_{-2.6}$	$-11^{+4.1}_{-1.4}$	-7.7 ± 9.2	-10.9 ± 3.0
$\bar{B}_s^0 \to K^{*0}\rho^0$	C	65.4	$59.1^{+10.4}_{-8.9}$	$62.7^{+15.7}_{-20.4}$	$46^{+23.4}_{-39.2}$	19.5 ± 23.5	4.9 ± 18.3
$\bar{B}_s^0 \to K^{*0}\omega$	C	-73.3	$-69.3^{+11.3}_{-10.6}$	$-78.1^{+17.6}_{-14.1}$	$-50^{+28.1}_{-17.2}$	-36.8 ± 40.1	32.2 ± 16.0
$\bar{B}_s^0 \to K^{*+}K^{*-}$	P	4.5	$6.8^{+5.4}_{-4.3}$	$8.8^{+2.6}_{-9.8}$	$21^{+2.2}_{-4.5}$	20.6 ± 23.3	21.1 ± 7.1
$\bar{B}_s^0 \to \omega\phi$	P	23.5	$-22.1^{+1.0}_{-1.0}$	$28.0^{+4.9}_{-8.2}$	$-8^{+20.2}_{-15.1}$	0	-15.0 ± 7.0
$\bar{B}_s^0 \to \rho^0\phi$	P	18.7	$39.6^{+3.6}_{-3.1}$	$-4.3^{+1.9}_{-1.3}$	$83^{+10.1}_{-3.6}$	0	0
$\bar{B}_s^0 \to \rho^+\rho^-$	A	-2.1	$-0.4^{+0.5}_{-0.3}$	$-2.9^{+1.6}_{-1.7}$	0	–	0
$\bar{B}_s^0 \to \rho^0\rho^0$	A	-2.1	$-0.4^{+0.5}_{-0.3}$	$-2.9^{+1.6}_{-1.7}$	0	–	0
$\bar{B}_s^0 \to \omega\omega$	A	-1.9	$-0.4^{+0.5}_{-0.3}$	$-3.3^{+1.8}_{-1.7}$	0	–	0
$\bar{B}_s^0 \to \omega\rho^0$	A	7.3	$5.8^{+3.2}_{-3.4}$	$11.1^{+2.7}_{-6.6}$	0	–	0

Table 9
Transverse polarization fractions $f_\perp$ (%), and relative phase $\phi_\parallel$ (rad) and $\phi_\perp$ (rad) in the $\bar{B}_s^0 \to VV$ decays calculated in the PQCD approach.

Decay mode	$f_\perp$ (%)		$\phi_\parallel$ (rad)		$\phi_\perp$ (rad)	
	LO	NLO	LO	NLO	LO	NLO
$\bar{B}_s^0 \to \rho^- K^{*+}$	3.2	$2.8^{+0.23}_{-0.45}$	3.21	$3.12^{+0.08}_{-0.06}$	3.21	$3.18^{+0.03}_{-0.05}$
$\bar{B}_s^0 \to \rho^0 K^{*0}$	26.2	$8.9^{+2.1}_{-1.9}$	1.63	$1.50^{+0.64}_{-0.12}$	1.63	$1.54^{+0.41}_{-0.11}$
$\bar{B}_s^0 \to \omega K^{*0}$	25.4	$8.9^{+0.05}_{-0.05}$	2.38	$1.85^{+0.05}_{-0.05}$	2.45	$1.94^{+0.05}_{-0.05}$
$\bar{B}_s^0 \to K^{*+}K^{*-}$	27.3	$23.9^{+4.4}_{-5.2}$	2.79	$2.34^{+0.13}_{-0.10}$	2.83	$2.39^{+0.30}_{-0.22}$
$\bar{B}_s^0 \to \omega\phi$	17.3	$38.6^{+5.6}_{-3.2}$	2.93	$3.12^{+0.23}_{-0.12}$	2.92	$3.10^{+0.25}_{-0.13}$
$\bar{B}_s^0 \to \rho^0\phi$	7.8	$4.4^{+1.5}_{-1.1}$	2.52	$2.41^{+0.07}_{-0.05}$	2.50	$2.67^{+0.05}_{-0.04}$
$\bar{B}_s^0 \to \rho^+\rho^-$	~ 0	~ 0	3.42	$3.35^{+0.21}_{-0.16}$	3.02	$2.67^{+0.15}_{-0.20}$
$\bar{B}_s^0 \to \rho^0\rho^0$	~ 0	~ 0	3.42	$3.35^{+0.21}_{-0.16}$	3.02	$2.67^{+0.15}_{-0.20}$
$\bar{B}_s^0 \to \rho^0\omega$	~ 0	~ 0	3.38	$3.28^{+0.05}_{-0.03}$	2.34	$2.02^{+0.15}_{-0.14}$
$\bar{B}_s^0 \to \omega\omega$	~ 0	~ 0	3.41	$3.13^{+0.18}_{-0.24}$	3.05	$2.66^{+0.16}_{-0.13}$

and $B_s^0 \to K^{*0}\bar{K}^{*0}$, imply the destructive interferences induced by the significant $SU(3)$ flavor symmetry-breaking effects, which made the $Br(B_s^0 \to K^{*0}\bar{K}^{*0})$ smaller than the $Br(B_s^0 \to \phi\phi)$ with a factor about 3, while the difference of the measured decay rates is around a factor of two as shown in Table 1.

(2) From the Table 1, one can find that, the NLO contributions such as Wilson coefficients at NLO level, the vertex corrections, the quark loop effects can provide the evident enhancements to the $\bar{B}_s^0 \to \phi\phi$, $K^{*0}\phi$ and $\bar{B}_s^0 \to \bar{K}^{*0}K^{*0}$ decays, while the chromo-magnetic penguin contributions lead to the small reduction to their decay rates. Furthermore, the quark loop effects largely increase the numerical results of the branching ratios of the considered

Table 10
The relative phases $\Delta\phi_\parallel$ (10^{-2} rad), $\Delta\phi_\perp$ (10^{-2} rad), and the CP asymmetry parameters A^0_{CP} (%) and $A^\perp_{CP}$ (%) in the $\bar{B}^0_s \to VV$ decays calculated in the LO and NLO PQCD approach.

Decay mode	A^0_{CP} (%)		$A^\perp_{CP}$ (%)		$\Delta\phi_\parallel$ (10^{-2} rad)		$\Delta\phi_\perp$ (10^{-2} rad)	
	LO	NLO	LO	NLO	LO	NLO	LO	NLO
$\bar{B}^0_s \to \phi\phi$	0	$0.5^{+0.5}_{-0.3}$	0	$-0.3^{+0.2}_{-0.6}$	0	~ 0	0	~ 0
$\bar{B}^0_s \to K^{*0}\phi$	0	$-6.3^{+1.8}_{-1.4}$	0	$5.8^{+2.1}_{-2.4}$	~ 0	$-5.4^{+1.9}_{-1.4}$	~ 0	$-4.8^{+2.9}_{-2.4}$
$\bar{B}^0_s \to \bar{K}^{*0}K^{*0}$	0	$0.3^{+0.2}_{-0.2}$	0	$-0.2^{+0.3}_{-0.2}$	0	~ 0	0	~ 0
$\bar{B}^0_s \to \rho^- K^{*+}$	-3.6	$-4.4^{+0.6}_{-0.7}$	50.1	$64.6^{+8.2}_{-8.3}$	11.3	$15.5^{+3.7}_{-3.3}$	10.0	$13.5^{+4.3}_{-2.4}$
$\bar{B}^0_s \to \rho^0 K^{*0}$	-18.3	$-11.2^{+6.1}_{-5.7}$	20.3	$35.3^{+7.2}_{-9.5}$	-31.1	$-20.6^{+45.3}_{-11.1}$	-35.4	$-22.3^{+54.1}_{-13.2}$
$\bar{B}^0_s \to \omega K^{*0}$	-9.6	$-7.7^{+5.3}_{-6.3}$	10.8	$28.2^{+7.2}_{-5.3}$	24.5	$29.3^{+9.3}_{-8.9}$	28.3	$15.5^{+11.6}_{-6.7}$
$\bar{B}^0_s \to K^{*+}K^{*-}$	37.1	$34.8^{+17.2}_{-16.3}$	-28.2	$-23.4^{+2.4}_{-2.2}$	65.5	$44.2^{+6.1}_{-5.8}$	65.7	$44.2^{+5.1}_{-4.2}$
$\bar{B}^0_s \to \omega\phi$	-2.3	$-12.8^{+2.6}_{-4.3}$	5.9	$20.1^{+3.4}_{-2.1}$	-33.5	$-31.5^{+9.5}_{-11.3}$	-34.5	$-31.5^{+12.3}_{-12.6}$
$\bar{B}^0_s \to \rho^0\phi$	4.5	$7.6^{+3.6}_{-3.1}$	-25.6	$-35.4^{+6.8}_{-6.4}$	-52.1	$-44.5^{+7.2}_{-6.7}$	-55.1	$-42.3^{+11.2}_{-8.8}$
$\bar{B}^0_s \to \rho^+\rho^-$	0.0	0.0	25.2	$35.5^{+7.9}_{-5.1}$	2.8	$1.8^{+0.4}_{-0.8}$	-27.1	$-44.1^{+4.5}_{-3.6}$
$\bar{B}^0_s \to \rho^0\rho^0$	0.0	0.0	25.2	$35.5^{+7.9}_{-5.1}$	2.8	$1.8^{+0.4}_{-0.8}$	-27.1	$-44.1^{+4.5}_{-3.6}$
$\bar{B}^0_s \to \rho^0\omega$	0.0	0.0	33.3	$21.6^{+5.8}_{-4.6}$	-10.0	$-12.5^{+3.3}_{-3.8}$	-28.3	$-23.4^{+7.1}_{-8.1}$
$\bar{B}^0_s \to \omega\omega$	0.0	0.0	23.9	$36.2^{+6.8}_{-4.6}$	2.5	$1.8^{+0.5}_{-0.5}$	-30.5	$-44.5^{+3.9}_{-4.4}$

three modes because of the possible constructive interferences between the tree and penguin amplitudes. However, the total enhancements to the branching ratios due to the inclusion of all known NLO corrections are not very large: less than 35% in magnitude. Anyway, the consistency between the theory and the data for the decay rates of the two $\Delta S = 1$ modes are improved and the predictions at NLO level agree with the current measurements within uncertainties. It is worth emphasizing that, for the $\Delta D = 1$ $\bar{B}^0_s \to K^{*0}\phi$ decay, the NLO PQCD prediction for its branching fraction is still much smaller than the present data, however, it agrees well with those in different theoretical approaches/methods such as QCDF, SCET, and FAT within errors, which can be seen explicitly in Table 1. It is expected that the combined analyses from the updated LHCb and Belle-II measurements in the near future would help to clarify this discrepancy.

(3) For $B^0_s \to \bar{K}^{*0}K^{*0}$ decay, the PQCD predictions for f_L and $f_\perp$ will become a bit large (small) after the inclusion of the NLO contributions, but still be consistent with previous theoretical predictions based on QCDF, SCET and FAT, even with those measured ones, since both theoretical and experimental errors are still rather large in magnitude. For $B^0_s \to \phi\phi$ and $B^0_s \to \phi\bar{K}^{*0}$ decays, fortunately, it is more interesting to observe that the NLO contributions to f_L and $f_\perp$ are very small in size, while the PQCD predictions for both f_L and $f_\perp$ agree well with other theoretical predictions, and with those measured values as well.

(4) As we know, the annihilation diagrams can play important roles in the investigations of heavy flavor system, although these contributions are generally power suppressed. As mentioned in the Introduction, the weak penguin annihilation contributions can be considered as one of the strategies to explain the "polarization puzzle". In fact, when the annihilation amplitudes are turned off in the decays of $\bar{B}^0_s \to \phi\phi, K^{*0}\phi$ and $\bar{B}^0_s \to \bar{K}^{*0}K^{*0}$, all the branching ra-

tios will decrease about 60%, 64%, and 27%, respectively, which could be easily inferred from the Table 3. Correspondingly, without the annihilation contributions, the longitudinal-polarization-dominance really exhibits, which suggests that the annihilation contributions in these penguin-dominated B_s decay modes could indeed enhance the transverse polarization fractions and reduce the longitudinal ones simultaneously with different extent. Of course, more stringent constraints on the theoretical uncertainties arising from the nonperturbative hadronic parameters are urgently demanded. Although the predictions look roughly consistent with the current measurements within still large theoretical errors, it should be noted that the annihilation amplitudes might not be the only source to explain the dramatically small $f_L(B_s^0 \to \bar{K}^0 K^{*0})$, if the significantly large differences between the theory and the experiment always exists as given in the Table 2.

(5) Moreover, the direct *CP* asymmetries and the relative phases of the decays of $\bar{B}_s^0 \to \phi\phi, K^{*0}\phi$ and $\bar{B}_s^0 \to \bar{K}^{*0}K^{*0}$ are also studied in the PQCD approach with inclusion of the currently known NLO contributions. Because these considered modes are induced only by penguin operators, their direct *CP*-violations are naturally zero without the interferences between the tree and penguin amplitudes in PQCD approach at LO, as listed in Table 5. After the inclusion of the NLO contributions, their direct CP asymmetries are nonzero but still very small: $(0.7 \pm 0.2)\%$, $(-15.9^{+2.7}_{-2.0})\%$, and $(0.7 \pm 0.2)\%$ respectively, which are comparable with the results of QCDF [3] ($(0.2^{+0.6}_{-0.4})\%$, $(-9^{+5}_{-6})\%$, and $(0.4^{+1.0}_{-0.6})\%$) and SCET [10] ($(-0.39 \pm 0.44)\%$, $(6.6 \pm 7.6)\%$, and $(-0.56 \pm 0.61)\%$) but with an overall opposite sign to those in SCET. In light of the relative phases, the NLO PQCD predictions of $\phi_\parallel$ and $\phi_\perp$ of the $B_s^0 \to \phi\phi$ mode are a bit smaller than the measured one, which would be further studied in the future. The numerical results for other relative phases would be tested by the near future experiments.

We now turn to study the remaining ten $B_s \to VV$ decays that have not been measured experimentally. In Table 6, we present our LO and NLO PQCD predictions for the CP-averaged branching ratios of the ten $\bar{B}_s^0 \to VV$ decay modes. We also classify these modes with different dominant topologies such as "T", "C", "A", etc. We find numerically that:

(1) Explicitly, the ten $B_s^0 \to VV$ decays as listed in Table 6 can be classified into three types: (a) the one "T" decay $\bar{B}_s^0 \to \rho^- K^{*+}$ and two "C" decays $\bar{B}_s^0 \to (\rho^0, \omega)K^{*0}$; (b) three "P" decays $\bar{B}_s^0 \to K^{*+}K^{*-}$ and $\bar{B}_s^0 \to (\rho^0, \omega)\phi$ modes; and (c) four pure weak annihilation "A" decays $\bar{B}_s^0 \to (\rho, \omega)(\rho, \omega)$. In fact, we here have reproduced the predictions of the branching ratios as given in Ref. [9] with PQCD approach at LO independently. The slightly small deviations appeared in the Table 6 are induced by some updated input parameters, such as the decay constants and the CKM matrix elements.

(2) For $\bar{B}_s^0 \to \rho^- K^{*+}$ decay, its LO decay rate will decrease around 10% after inclusion of the known NLO corrections due to less sensitivity to the vertex corrections. Hence, the NLO PQCD prediction of $Br(\bar{B}_s^0 \to \rho^- K^{*+})$ is still consistent with those in the QCDF, SCET, even FAT approaches within the theoretical uncertainties. However, because the "C" channels are highly sensitive to the vertex corrections with a large imaginary amplitude to the factorizable emission diagrams, the $\bar{B}_s^0 \to \rho^0 K^{*0}$ and ωK^{*0} decay rates receive significant enhancements with a factor around 2, which can be seen clearly in the Table 6 and agree with those estimated in other approaches such as QCDF, SCET, and FAT in general. Moreover, the relation of $Br(\bar{B}_s^0 \to \rho^0 K^{*0}) \sim Br(\bar{B}_s^0 \to \omega K^{*0})$ is induced by adopting the same QCD

behavior of the ρ^0 and ω states and similar decay constants and meson masses, which can be observed from the input parameters in Eqs. (15) and (30).

(3) For the decays of $\bar{B}_s^0 \to \omega\phi, \rho^0\phi$ and $\bar{B}_s^0 \to K^{*+}K^{*-}$, only the measured decay rate $Br(\bar{B}_s^0 \to \rho^0\phi) = (0.27 \pm 0.08) \times 10^{-6}$ from LHCb [17] is available now. From Table 6, one can see easily that the predicted branching ratio in the PQCD approach at the LO and NLO level agrees well with the data. Of course, all the available predictions for the $Br(B_s^0 \to \rho^0\phi)$ in the framework of the QCD-based factorization approaches also be consistent with the experimental measurements within the errors. However, the prediction based on the FAT is much smaller. It is more interesting to find that different patterns between $Br(B_s^0 \to \rho^0\phi)$ and $Br(B_s^0 \to \omega\phi)$ have been predicted in various frameworks: the moderate interferences between the $\bar{u}u$ and $\bar{d}d$ components in the ρ and ω mesons result in the relation of $Br(B_s^0 \to \rho^0\phi) \sim Br(B_s^0 \to \omega\phi)$ in PQCD_{LO}, PQCD_{NLO}, and QCDF, respectively, but the strong effects with different destructive and/or constructive interferences lead to the relations of $Br(B_s^0 \to \rho^0\phi)_{\text{SCET}} \gg Br(B_s^0 \to \omega\phi)_{\text{SCET}}$ and $Br(B_s^0 \to \rho^0\phi)_{\text{FAT}} \ll Br(B_s^0 \to \omega\phi)_{\text{FAT}}$. Moreover, the improved NLO PQCD prediction of $Br(B_s^0 \to K^{*+}K^{*-})$ is also consistent with that provided by other approaches/methods. These phenomenologies would be tested in the near future at the LHCb and Belle-II experiments by measuring the $Br(B_s^0 \to \omega\phi)$ with good precision.

(4) For the four pure annihilation decays $\bar{B}_s^0 \to (\rho^+\rho^-, \rho^0\rho^0, \rho^0\omega, \omega\omega)$, in fact, the NLO correction comes only from the usage of the NLO Wilson coefficients $C_i(\mu)$ and the strong coupling constant $\alpha_s(\mu)$ at the two-loop level, which result in negligible corrections to the $Br(B_s^0 \to \rho^0\omega)$ and $Br(B_s^0 \to \rho^+\rho^-)$ while around 10% enhancement to the $Br(B_s^0 \to \rho^0\rho^0)$ and $Br(B_s^0 \to \omega\omega)$. It should be mentioned that the annihilation diagrams in the QCDF and SCET framework have to be fitted from the experimental measurements because of the endpoint singularities. While, in Ref. [10], the authors neglected the contributions arising from the annihilation diagrams based on the arguments of the $\mathcal{O}(1/m_B)$ power-suppressed effects. The very different results in the FAT method from those in the PQCD and QCDF approaches should be examined by the near future measurements at LHC and Belle-II experiments. It is worth emphasizing that the pure annihilation $B_s^0 \to \pi^+\pi^-$ decay rate has been confirmed by the CDF and LHCb collaborations. Therefore, these large branching ratios of the $B_s^0 \to \rho^+\rho^-$, $\rho^0\rho^0$, and $\omega\omega$ modes are expected to be verified soon. Moreover, the substantial cancelations between the contributions arising from the $\bar{u}u$ and $\bar{d}d$ components of the ρ^0 and ω mesons result in the tiny decay rate of the $B_s^0 \to \rho^0\omega$ mode, which would be examined in the future.

Next, we turn to discuss the longitudinal polarization fractions f_L of the remaining ten $B_s \to VV$ decays. From the numerical results as given in Table 7, one can see that:

(1) Generally speaking, except for the $B_s^0 \to K^{*+}K^{*-}$ and $B_s^0 \to \omega\phi$ channels, most of these considered ten $B_s^0 \to VV$ decays are governed by the longitudinal amplitudes by including the known NLO corrections in the PQCD approach, in which (a) the $B_s^0 \to K^{*0}(\rho^0, \omega)$ decays do receive significant enhancements to f_L, then both of the fractions are increased from around 50% to about 80% and consistent with those predicted in the QCDF, SCET, and FAT within errors; (b) the four pure annihilation $B_s^0 \to (\rho^+\rho^-, \rho^0\rho^0, \rho^0\omega, \omega\omega)$ decays are absolutely dominated by the longitudinal polarization contributions, therefore, the fractions of these four modes are around 100%.

(2) For the penguin-dominated $\bar{B}_s^0 \to K^{*+}K^{*-}$ decay, we find a small LO PQCD prediction $f_L \perp\sim 0.4$, as presented in the Table 7. When the NLO contributions are taken into account, f_L will become a little larger to around 0.48. It is interesting to note that the significant transverse-components dominance have been obtained in various approaches such as QCDF, SCET, and FAT, which could be examined in the near future by experiments associated with the large decay rates predicted in the aforementioned approaches.
(3) For the pure emission decay of $\bar{B}_s^0 \to \omega\phi$, the longitudinal polarization fraction f_L is around 55% in the PQCD approach at NLO level, because the $(S-P)(S+P)$ densities in the hard spectator scattering diagrams together with the NLO contributions can provide the sizable transverse polarization contributions. By considering the very large theoretical errors, the relation $f_L \sim (f_\parallel + f_\perp)$ might be got in the framework of QCDF. However, it is highly different from that provided in SCET, namely, 100%. The future stringent tests from the experimental measurements would help us to distinguish these theoretical approaches. Of course, it seems not easy because of the predicted small branching ratios around $10^{-7} \sim 10^{-8}$ in various approaches.

For the direct CP asymmetries of the considered $\bar{B}_s^0 \to VV$ decays collected in Table 5 and 8, we have some comments as follows:

(1) In fact, the LO PQCD predictions for the direct *CP* asymmetries of the decays of $B_s^0 \to VV$ obtained in this paper do agree very well with those as given in Ref. [9], except for the $\bar{B}_s^0 \to \rho^0\phi$ channel. Due to the different choices of the updated input parameters, the sensitivity of the direct *CP* violation to the adopted parameters can be observed in the $B_s^0 \to \rho^0\phi$ mode, and finally the result has an opposite sign to that in the previous LO PQCD calculations, which demands the tests from the experiments at LHCb and Belle-II.
(2) Generally speaking, except for the penguin-dominated $B_s^0 \to \rho^0\phi, \omega\phi$ and $B_s^0 \to K^{*0}\phi$ modes, the effects of the NLO contributions to the direct *CP* asymmetries are not significant in magnitude for most of the $\bar{B}_s^0 \to VV$ decays. Specifically, for the $\bar{B}_s^0 \to \omega\phi$ decay, the PQCD prediction of the $\mathcal{A}_{CP}^{\rm dir}$ can vary from 20% to -20%, after the inclusion of the NLO corrections, which is because an extra strong phase appears in the decay amplitudes from the factorizable emission diagrams. For the $\bar{B}_s^0 \to \rho^0\phi$ decay, on the other hand, the NLO contributions to the $\mathcal{A}_{CP}^{\rm dir}$ in magnitude can be found with a factor around 2, relative to the LO PQCD prediction, which indicates a possibly constructive interference between the tree and penguin amplitudes after the inclusion of the NLO vertex corrections. All the predictions of the $A_{CP}^{\rm dir}(B_s^0 \to K^{*0}\phi)$ in various approaches are generally consistent within large theoretical uncertainties, which could be tested by the future measurements.
(3) For the two "Color-suppressed" decays $\bar{B}_s^0 \to K^{*0}\rho^0$ and $\bar{B}_s^0 \to K^{*0}\omega$, because of the large penguin contributions from the chirally enhanced annihilation diagrams, which are at the same level as the tree contributions from the emission diagrams, this sizable interference between the tree and penguin contributions makes the direct CP asymmetries as large as $60\% \sim 70\%$ but with an opposite sign for these two channels.
(4) By comparing the numerical results as listed in the fifth to seventh columns of Table 8, due to the different origins of the strong phase, one can see that the PQCD, QCDF, and SCET predictions for the CP asymmetries of the considered decays are indeed quite different. As is well known, besides the weak CKM phases, the direct CP asymmetries also depend on the strong phase. In SCET, the strong phase is only from the nonperturbative charming penguin at leading power and leading order; while in the QCDF and PQCD approach, the strong

phase comes from the hard spectator scattering and annihilation diagrams respectively. The forthcoming LHCb and Belle-II measurements for these direct *CP* violations can help us to differentiate these factorization approaches.

(5) The direct *CP*-violating asymmetries, the relative phases, and the differences of the relative phases in different polarizations for the considered $B_s^0 \to VV$ decays have not been measured experimentally to date yet, neither reported in other approaches by the colleagues theoretically. All these predictions in the PQCD approach at NLO level have to await for the future confirmations arising from both of the theoretical and experimental sides.

In Table 9 and 10, we listed the LO and NLO PQCD predictions for the transverse polarization fractions $f_\perp$, the relative phase $\phi_\parallel$ and $\Delta\phi_\parallel$, $\phi_\perp$ and $\Delta\phi_\perp$, and the CP asymmetry parameters A_{CP}^0 (%) and $A_{CP}^\perp$ (%), for the considered $\bar{B}_s^0 \to VV$ decays. It is easy to see that the NLO contributions to all these physics parameters are small or moderate in magnitude. All these PQCD predictions could be tested in the near future by the forthcoming LHCb and Belle-II experiments.

4. Summary

In this work, we studied the two-body charmless hadronic decays $\bar{B}_s^0 \to VV$ (here $V = (\rho, K^*, \phi, \omega)$) by employing the PQCD factorization approach with the inclusion of all currently known NLO contributions, such as the NLO vertex corrections, the quark loop effects and the chromo-magnetic penguin diagrams etc. We focus on the examination for the effects of those NLO contributions to the *CP*-averaged branching ratios, the *CP*-violating asymmetries, the polarization fractions and other physical observables of the thirteen $\bar{B}_s^0 \to VV$ decay modes.

By the numerical evaluations and the phenomenological analyses, we found the following interesting points:

(1) For the measured $B_s^0 \to \phi\phi$, $K^{*0}\phi$ and $\bar{K}^{*0}K^{*0}$ decays, the agreement between the PQCD predictions for the CP-averaged branching ratios and the measured vales are improved effectively after the inclusion of the NLO contributions. For $B_s^0 \to K^{*0}\phi$ decay, although there exists a clear difference between the central value the NLO PQCD prediction for its CP-averaged branching ratio ($(0.42^{+0.13}_{-0.10}) \times 10^{-6}$) and the measured one ($(1.13 \pm 0.30) \times 10^{-6}$), but they are still consistent within 3σ, due to the still large experimental errors.

(2) For the measured $B_s^0 \to \phi\phi$, $K^{*0}\phi$ and $\bar{K}^{*0}K^{*0}$ decays, the NLO corrections to the PQCD predictions for the longitudinal and transverse polarization fractions (f_L, $f_\perp$), the relative phases ($\phi_\parallel$, $\phi_\perp$) are small in size. The NLO PQCD predictions for these physical observables do agree with those from the QCDF, SCET and FAT approaches, and also agree well with those currently available experimental measurements. It is easy to see from the results as listed in Table 3 that the weak penguin annihilation contributions play an important role in understanding the data about the decay rates, f_L and $f_\perp$ for three measured decays.

(3) For $B_s^0 \to \rho^0\phi$ decay, furthermore, the NLO PQCD prediction for its branching ratio does agree very well with the measured one as reported by LHCb Collaboration very recently [17].

(4) For other considered $B_s^0 \to VV$ decays, the NLO PQCD predictions for the decay rates and other physical observables studied in this paper are also basically consistent with other theoretical predictions obtained based on QCDF, SCET and FAT approaches/methods. The future measurements with good precision could be employed to test or examine the differences

among these rather different approaches. Of course, the still missing NLO contributions in the PQCD approach are the urgent meanwhile challenging works to be completed.

Acknowledgements

This work is supported by the National Natural Science Foundation of China under Grants No. 11775117, 11765012 and 11235005, by the Qing Lan Project of Jiangsu Province, and by the Research Fund of Jiangsu Normal University under Grant No. HB2016004.

References

[1] X.Q. Li, G.R. Lu, Y.D. Yang, Charmless $B_s \to VV$ decays in QCD factorization, Phys. Rev. D 68 (2003) 114015.
[2] M. Beneke, J. Rohrer, D.S. Yang, Branching fractions, polarisation and asymmetries of $B \to VV$ decays, Nucl. Phys. B 774 (2007) 64.
[3] H.Y. Cheng, C.K. Chua, QCD factorization for charmless hadronic B_s decays revisited, Phys. Rev. D 80 (2009) 114026.
[4] Q. Chang, X.N. Li, X.Q. Li, J.F. Sun, Study of the weak annihilation contributions in charmless $B_s \to VV$ decays, Eur. Phys. J. C 77 (2017) 415.
[5] M. Bartsch, G. Buchalla, C. Kraus, $B_s \to V_L V_L$ decays at next-to-leading order in QCD, arXiv:0810.0249 [hep-ph].
[6] Y.H. Chen, H.Y. Cheng, B. Tseng, Charmless hadronic two-body decays of B_s mesons, Phys. Rev. D 59 (1999) 074003.
[7] J. Zhu, Y.L. Shen, C.D. Lü, $B_s \to \rho(\omega)K^*$ with the perturbative QCD approach, J. Phys. G 32 (2006) 101.
[8] A. Ali, G. Kramer, Y. Li, C.D. Lü, Y.L. Shen, W. Wang, Y.M. Wang, Charmless nonleptonic B_s decays to PP, PV, and VV final states in the pQCD approach, Phys. Rev. D 76 (2007) 074018.
[9] Z.T. Zou, A. Ali, C.D. Lü, X. Liu, Y. Li, Improved estimates of the $B_{(s)} \to VV$ decays in perturbative QCD approach, Phys. Rev. D 91 (2015) 054033.
[10] C. Wang, S.H. Zhou, Y. Li, C.D. Lü, Global analysis of charmless B decays into two vector mesons in soft-collinear effective theory, Phys. Rev. D 96 (2017) 073004.
[11] C.W. Bauer, D. Pirjol, I.Z. Rothstein, I.W. Stewart, $B \to M_1 M_2$: factorization, charming penguins, strong phases, and polarization, Phys. Rev. D 70 (2004) 054015.
[12] T. Aaltonen, et al., CDF Collaboration, Measurement of polarization and search for CP-violation in $B_s^0 \to \phi\phi$ decays, Phys. Rev. Lett. 107 (2011) 261802.
[13] R. Aaij, et al., LHCb Collaboration, First observation of the decay $B_s^0 \to K^{*0}\bar{K}^{*0}$, Phys. Lett. B 709 (2012) 50.
[14] R. Aaij, et al., LHCb Collaboration, Measurement of CP asymmetries and polarisation fractions in $B_s^0 \to K^{*0}\bar{K}^{*0}$ decays, J. High Energy Phys. 07 (2015) 166.
[15] R. Aaij, et al., LHCb Collaboration, Measurement of the polarization amplitudes and triple product asymmetries in the $B_s^0 \to \phi\phi$ decay, Phys. Lett. B 713 (2012) 369.
[16] R. Aaij, et al., LHCb Collaboration, Measurement of the $B_s^0 \to \phi\phi$ branching fraction and search for the decay $B^0 \to \phi\phi$, J. High Energy Phys. 1510 (2015) 053.
[17] R. Aaij, et al., LHCb Collaboration, Observation of the decay $B_s^0 \to \phi\pi^+\pi^-$ and evidence for $B^0 \to \phi\pi^+\pi^-$, Phys. Rev. D 95 (2017) 012006.
[18] R. Aaij, et al., LHCb Collaboration, First observation of the decay $B_s^0 \to \phi\bar{K}^{*0}$, J. High Energy Phys. 11 (2013) 092.
[19] LHCb Collaboration, A. Bharucha, et al., Implications of LHCb measurements and future prospect, Eur. Phys. J. C 73 (2013) 2373.
[20] C. Patrignani, et al., Particle Data Group, Review of particle physics, Chin. Phys. C 40 (2016) 100001 and 2017 update.
[21] Y. Amhis, et al., Heavy Flavor Averaging Group, Averages of b-hadron, c-hadron, and τ-lepton properties as of summer 2016, Eur. Phys. J. C 77 (2017) 895, arXiv:1612.07233v2 [hep-ex].
[22] B. Aubert, et al., BABAR Collaboration, Rates, polarizations, and asymmetries in charmless vector–vector B meson decays, Phys. Rev. Lett. 91 (2003) 171802;
K.F. Chen, et al., Belle Collaboration, Measurement of branching fractions and polarization in $B \to \phi K^{(*)}$ decays, Phys. Rev. Lett. 91 (2003) 201801.
[23] J.G. Korner, G.R. Goldstein, Quark and particle helicities in hadronic charmed particle decays, Phys. Lett. B 89 (1979) 105.

[24] P. Colangelo, F. De Fazio, T.N. Pham, The riddle of polarization in $B \to VV$ transitions, Phys. Lett. B 597 (2004) 291.
[25] A. Gritsan, Polarization puzzle in $B \to \phi K^*$ and other $B \to VV$ at BABAR, arXiv:hep-ex/0409059;
W.S. Hou, M. Nagashima, Resolving the $B \to \phi K^*$ polarization anomaly, arXiv:hep-ph/0408007;
C.S. Kim, Y.D. Yang, Polarization anomaly in $B \to \phi K^*$ and probe of tensor interactions, arXiv:hep-ph/0412364.
[26] H.N. Li, Resolution to the $B \to \phi K^*$ polarization puzzle, Phys. Lett. B 622 (2005) 63.
[27] H.N. Li, S. Mishima, Polarizations in $B \to VV$ decays, Phys. Rev. D 71 (2005) 054025.
[28] B. Aubert, et al., BaBar Collaboration, Phys. Rev. Lett. 101 (2008) 161801.
[29] A.L. Kagan, Polarization in $B \to VV$ decays, Phys. Lett. B 601 (2004) 151.
[30] M. Ladisa, V. Laporta, G. Nardulli, P. Santorelli, Final state interactions for $B \to VV$ charmless decays, Phys. Rev. D 70 (2004) 114025.
[31] H.Y. Cheng, C.K. Chua, A. Soni, Final state interactions in hadronic B decays, Phys. Rev. D 71 (2005) 014030.
[32] S. Descotes-Genon, J. Matias, J. Virto, Analysis of $B_{d,s}$ mixing angles in the presence of new physics and an update of $B_s \to K^{*0}\bar{K}^{*0}$, Phys. Rev. D 85 (2012) 034010;
Y.D. Yang, R.M. Wang, G.R. Lu, Polarizations in decays $B_{u,d} \to VV$ and possible implications for R-parity violating supersymmetry, Phys. Rev. D 72 (2005) 015009;
P.K. Das, K.C. Yang, Data for polarization in charmless $B \to \phi K^*$: a signal for new physics?, Phys. Rev. D 71 (2005) 094002;
W.J. Zou, Z.J. Xiao, Charmless $B \to PV, VV$ decays and new physics effects in the minimal supergravity model, Phys. Rev. D 72 (2005) 094026.
[33] A. Giri, R. Mohanta, Searching for new physics in the angular distribution of $B_d^0 \to \phi K^{*0}$ decay, Phys. Rev. D 69 (2003) 014008;
S. Baek, A. Datta, P. Hamel, O.F. Hernandez, D. London, Polarization states in $B \to \rho K^*$ and new physics, Phys. Rev. D 72 (2005) 094008;
C.S. Huang, P. Ko, X.H. Wu, Y.D. Yang, MSSM anatomy of the polarization puzzle in $B \to \phi K^*$ decays, Phys. Rev. D 73 (2006) 034026;
S.S. Bao, F. Su, Y.L. Wu, C. Zhuang, Exclusive $B \to VV$ decays and CP violation in the general two-Higgs-doublet model, Phys. Rev. D 77 (2008) 095004.
[34] H.Y. Cheng, K.C. Yang, Branching ratios and polarization in $B \to VV, VA, AA$ decays, Phys. Rev. D 78 (2008) 094001;
H.Y. Cheng, K.C. Yang, Revisiting charmless hadronic $B_{u,d}$ decays in QCD factorization, Phys. Rev. D 80 (2009) 114008.
[35] Y. Li, C.D. Lü, Branching ratio and polarization of $B \to \rho(\omega)\rho(\omega)$ decays in perturbative QCD approach, Phys. Rev. D 73 (2006) 014024;
H.W. Huang, C.D. Lü, T. Morii, Y.L. Shen, G.L. Song, J. Zhu, Study of $B \to K^*\rho$, $K^*\omega$ decays with polarization in the perturbative QCD approach, Phys. Rev. D 73 (2006) 014011.
[36] J. Zhu, Y.L. Shen, C.D. Lü, Polarization, CP asymmetry, and branching ratios in $B \to K^*K^*$ with the perturbative QCD approach, Phys. Rev. D 72 (2005) 054015;
J. Zhu, Y.L. Shen, C.D. Lü, $B^0 \to \phi\phi$ decay in perturbative QCD approach, Eur. Phys. J. C 41 (2005) 311.
[37] C.H. Chen, Y.Y. Keum, H.N. Li, Perturbative QCD analysis of $B \to \phi K^*$ decays, Phys. Rev. D 66 (2002) 054013.
[38] H.N. Li, S. Mishima, Implication of the $B \to \rho\rho$ data on the $B \to \pi\pi$ puzzle, Phys. Rev. D 73 (2005) 114014.
[39] H.N. Li, S. Mishima, A.I. Sanda, Resolution to the $B \to \pi K$ puzzle, Phys. Rev. D 72 (2005) 114005.
[40] W. Bai, M. Liu, Y.Y. Fan, W.F. Wang, S. Cheng, Z.J. Xiao, Revisiting $K\pi$ puzzle in the pQCD factorization approach, Chin. Phys. C 38 (2014) 033101.
[41] Y.Y. Fan, W.F. Wang, S. Cheng, Z.J. Xiao, Anatomy of $B \to K\eta^{(\prime)}$ decays in different mixing schemes and effects of NLO contributions in the perturbative QCD approach, Phys. Rev. D 87 (2013) 094003.
[42] Z.J. Xiao, Z.Q. Zhang, X. Liu, L.B. Guo, Branching ratios and CP asymmetries of $B \to K\eta^{(\prime)}$ decays in the perturbative QCD approach, Phys. Rev. D 78 (2008) 114001.
[43] J.J. Wang, D.T. Lin, W. Sun, Z.J. Ji, S. Cheng, Z.J. Xiao, $\bar{B}_s^0 \to K\pi, KK$ decays and effects of the next-to-leading order contributions, Phys. Rev. D 89 (2014) 074046.
[44] Z.J. Xiao, Ya Li, D.Q. Lin, Y.Y. Fan, A.J. Ma, $B_s^0 \to (\pi\eta^{(\prime)}, \eta^{(\prime)}\eta^{(\prime)})$ decays and the effects of NLO contributions in pQCD, Phys. Rev. D 90 (2014) 114028.
[45] D.C. Yan, P. Yang, X. Liu, Z.J. Xiao, Anatomy of $B_s \to PV$ decays and effects of next-to-leading order contributions in the perturbative QCD factorization approach, Nucl. Phys. B 931 (2018) 79.
[46] H.N. Li, QCD aspects of exclusive B meson decays, Prog. Part. Nucl. Phys. 51 (2003) 85 and references therein.
[47] K.C. Bowler, L. DelDebbio, J.M. Flynn, L. Lellouch, V. Lesk, C.M. Maynard, J. Nieves, D.G. Richards, Improved $B \to \pi l \nu_l$ form factors from the lattice, Phys. Lett. B 486 (2000) 111.

[48] P. Ball, $B \to \pi$ and $B \to K$ transitions from QCD sum rules on the light-cone, J. High Energy Phys. 09 (1998) 005; P. Ball, Theoretical update of pseudoscalar meson distribution amplitudes of higher twist: the nonsinglet case, J. High Energy Phys. 01 (1999) 010.
[49] P. Ball, V.M. Braun, Y. Koike, K. Tanaka, Higher twist distribution amplitudes of vector mesons in QCD: formalism and twist 3 distributions, Nucl. Phys. B 529 (1998) 323.
[50] P. Ball, V.M. Braun, Higher twist distribution amplitudes of vector mesons in QCD: twist-4 distributions and meson mass corrections, Nucl. Phys. B 543 (1999) 201;
P. Ball, R. Zwicky, $B_{d,s} \to \rho, \omega, K^*, \phi$ decay form factors from light-cone sum rules reexamined, Phys. Rev. D 71 (2005) 014029.
[51] P. Ball, G.W. Jones, Twist-3 distribution amplitudes of K^* and ϕ mesons, J. High Energy Phys. 03 (2007) 069.
[52] G. Buchalla, A.J. Buras, M.E. Lautenbacher, Weak decays beyond leading logarithms, Rev. Mod. Phys. 68 (1996) 1125.
[53] R. Zhou, X.D. Gao, C.D. Lü, Revisiting the $B \to \pi\rho, \pi\omega$ decays in the perturbative QCD, Eur. Phys. J. C 72 (2012) 1923.
[54] Z.Q. Zhang, Z.J. Xiao, NLO contributions to $B \to K K^*$ decays in the pQCD approach, Eur. Phys. J. C 59 (2009) 49.
[55] S. Mishima, A.I. Sanda, Calculation of magnetic penguin amplitudes in $B \to \phi K$ decays using PQCD approach, Prog. Theor. Phys. 110 (2003) 549.
[56] H.Y. Cheng, K.C. Yang, Charmless $B \to V V$ decays in QCD factorization: implications of recent $B \to \phi K^*$ measurement, Phys. Lett. B 511 (2001) 40.
[57] M. Beneke, M. Neubert, QCD factorization for $B \to P P$ and $B \to P V$ decays, Nucl. Phys. B 675 (2003) 333.
[58] C. Wang, Q.A. Zhang, Y. Li, C.D. Lü, Charmless $B_{(s)} \to V V$ decays in factorization-assisted topological-amplitude approach, Eur. Phys. J. C 77 (2017) 333.